AES 8102243
Final Report

APTECH engineering services, inc ENGINEERING CONSULTANTS

795 SAN ANTONIO ROAD • PALO ALTO • CALIFORNIA 94303 (415) 858 • 2863

A FRACTURE MECHANICS EVALUATION OF CORE SPRAY SPARGER INDICATIONS

Prepared by

Russell C. Cipolla
Warren P. McNaughton
John A. Hayward*

Aptech Engineering Services, Inc.
795 San Antonio Road
Palo Alto, California 94303

Prepared for

Boston Edison Company
Pilgrim Station
Rocky Hill Road
Plymouth, Massachusetts 02360

Attention: Mr. Joseph A. Nicholson

December 1982

*Mr. J. Hayward is now with Design Reliability Assoc., Mountain View, CA 94040

QUALITY ASSURANCE
VERIFICATION RECORD SHEET

TITLE: A Fracture Mechanics Evaluation of Core Spray Sparger Indications.

Originated by Russell C Cipolla 2/28/83

Russell C. Cipolla

Warren P. McNaughton

Approved and Verified by

Geoffrey R Egan

Quality Assurance Approval Jeffrey D. Byron 3/3/83

Jeffrey D. Byron

TABLE OF CONTENTS

ILLUSTRATIONS

TABLES

SYNOPSIS

Surface indications have been located in the core spray sparger of the Pilgrim Nuclear Power Station operated by the Boston Edison Company (BECO). The indications were found by visual inspection during a scheduled outage in January 1980. The results of an evaluation of the significance of those indications on the sparger integrity were presented to BECO in September and in November 1981, in Aptech Engineering Services Report AES-81-10-83, entitled, "Preliminary Report Structural Evaluations of the Pilgrim Station Core Spray Sparger Based Upon Results From the October 1981 Remote Visual Inspection." This report has been reissued with changes as a final report in December 1982. The present report provides detailed analytical and computational background to that report. It also quantifies the potential degradation of the sparger to perform its design function and estimates the expected remaining service life of the sparger as a function of the size and location of indications observed.

The indications have been divided into two general groups for purposes of this evaluation: (1) those indications near the weld regions and heat affected zones of various attachment weldments, and (2) those remote from welds. The following assumptions have been utilized in the analysis that was performed:

- The principles of linear elastic fracture mechanics (LEFM) are applicable for predicting subcritical crack growth.

- The cracking mechanism is intergranular stress corrosion cracking (IGSCC) and, hence, the life prediction analysis was based upon an IGSCC model.

- The flaw model is based upon the solution for a center cracked flat plate geometry under general varying stress conditions.

- The representation of the crack growth rate or velocity is primarily based on upperbound da/dt behavior (i.e., Type 304 stainless steel in the furnace sensitized condition and tested in water with 8 ppm O_2 at 550°F).

- Crack arrest is assumed when crack driving force (i.e., maximum stress intensity factor K_{max} vanishes ($K_{max} = 0$).

- The maximum stress level is limited to yield strength at 550°F ($\sigma_y = 23.7$ ksi).

The analysis performed shows that for the proposed stress state existing at these locations, a through-wall crack located away from the welds will arrest given "service" stresses less than 10 ksi tension. The arrest length is shorter than the critical size to cause failure by a limit load mechanism. A through-wall crack located in the region of the weld details, however, may not arrest prior to reaching critical length (~ 80% of pipe circumference) to failure, even for low primary stress loads. However, established maintenance criteria requires the placement of an external pipe clamp when a 180° crack indication is detected or predicted. Consequently, failure by primary loading exceeding the limit-load capacity will be mitigated.

Section 1
INTRODUCTION

During a scheduled maintenance outage in January 1980, a remote video inspection found indications in the core spray sparger of Boston Edison's Pilgrim Nuclear Power Station. Aptech Engineering Services was asked to participate in determining the significance of these indications and did so in a two part study. First, a digital enhancement technique was used to enhance videotape inspection records to determine the validity of the suspected indications. Second, once it was determined that probable cracks did in fact exist in the sparger, a fracture mechanics evaluation was performed. A preliminary report, "Structural Evaluation of the Pilgrim Station Core Spray Sparger Based on Results From the October 1981 Remote Visual Inspection," AES-81-10-83, was issued in November 1981 and included the inspection results and a summary of the fracture mechanics evaluations. This report has been subsequently reissued as a final report in December 1982 with some minor revisions. The details of that latter work are the subject of this report.

The work detailed herein had four objectives:

- To assess the significance of core spray sparger indications on the structural integrity of the sparger
- To estimate the expected remaining service life of the sparger given its present condition
- To quantify the potential degradation of the sparger to perform its design function

- To establish inspection acceptance criteria and develop a maintenance action plan (see Appendix)

The digital enhancements showed that probable cracks did exist in the sparger (1). For the purposes of analysis, the indications were classified into two distinct groups: (1) those indications that were associated with weld and weld heat affected zones, and (2) those indications that were away from the weld regions. Details of typical indication sizes that were detected by the visual examination are given in Section 5.

The effect that the indications may have on the structural integrity of the core spray sparger has been determined using the limiting condition that the indications behave like cracks. Several questions were examined as outlined in the flow diagram of Figure 1-1. Given the presence of a flaw (in the worst case a through-thickness crack), could a growing flaw be expected to arrest under the combined actions of residual stress plus service induced stress? If so, how large would the flaws be when this occurred and would this length flaw affect integrity? If not, how long would it take a crack to grow before it did affect integrity?

To answer these questions, each region was examined in detail. The stresses associated with each region were critiqued and are summarized in Section 3. This discussion includes residual stresses due to sparger fabrication (i.e., pipe rolling and welding), and postulated levels of service-induced stress. A summary of the results of an experimental program performed by Teledyne Engineering Services (TES) to measure the rolling fabrication stresses is also included in Section 3. The probable crack growth rates are discussed in Section 4. These rates are a function of the material condition (history of fabrication) and stress levels and have been the subject of much experimental work in the past five years. Section 6 presents the background for limit load analysis, as well as the numerical results in order to address the questions of sparger integrity. The results of the analysis are presented in Section 7.

BOSTON EDISON CORE SPRAY SPARGER
FRACTURE MECHANICS EVALUATION

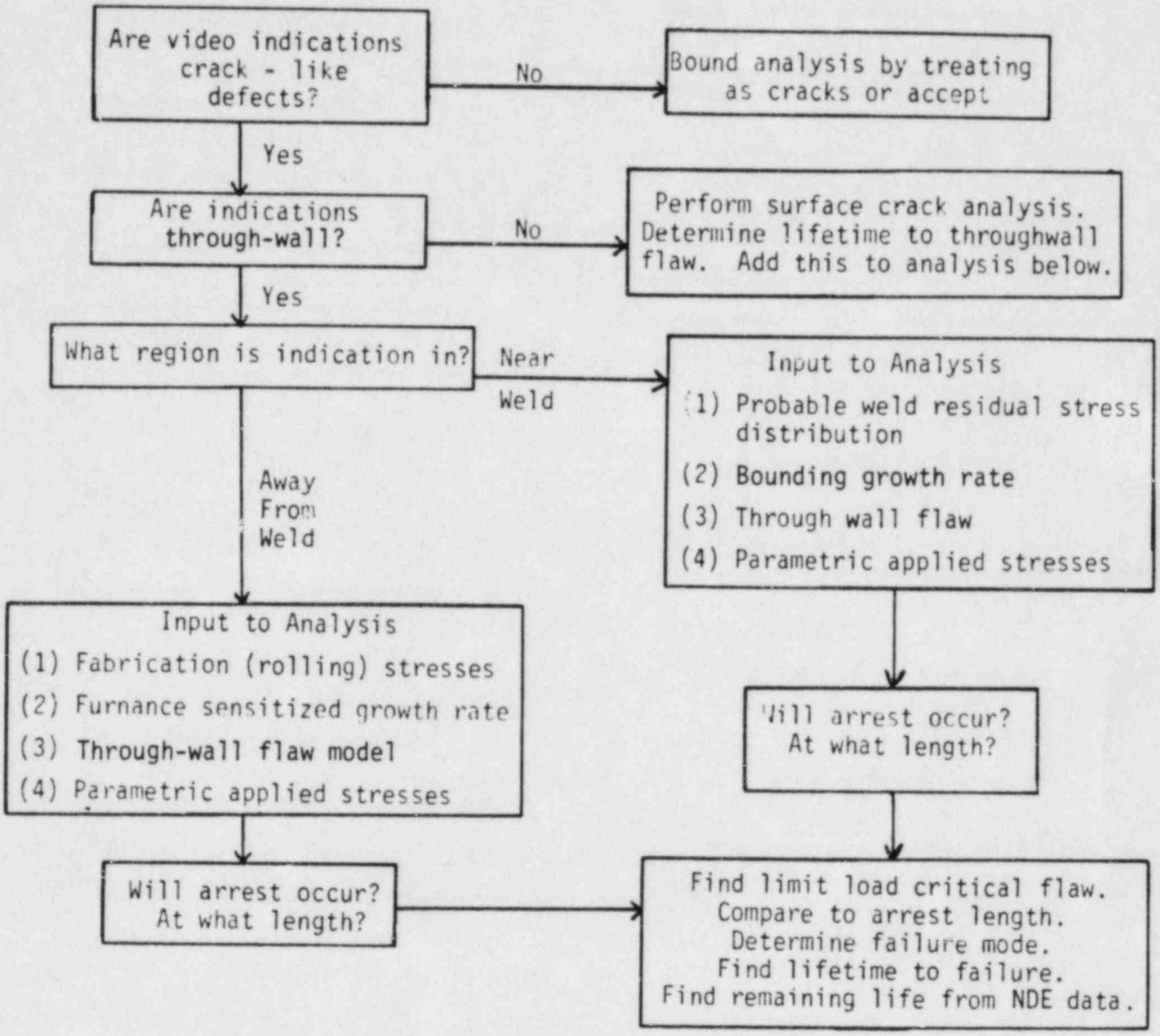

Figure 1-1

Before we proceed to the analytical assessment and numerical results, the next section (Section 2) presents the background and basis to the analytical methods and fracture mechanics concepts utilized throughout the remainder of the report.

Section 2
ANALYSIS METHOD

2.1 Introduction

In assessing the significance of sparger defects in stainless steel piping, two failure modes were investigated: (1) ultimate capacity or residual strength under increasingly long cracks, and (2) subcritical crack growth by an intergranular stress corrosion cracking (IGSCC) mechanism. The failure behavior of pipes under monotonic loading can be classified into three regimes in which a specific type of failure mode is appropriate. The disciplines required to assess these regimes are:

- Linear Elastic Fracture Mechanics (LEFM) - The structure fails in a brittle manner and, on a macroscale, the load to failure occurs within nominally elastic loading.

- Elastic-Plastic Fracture Mechanics (EPFM) - The structure fails in a ductile manner, and significant stable crack extension by tearing may precede ultimate failure.

- Fully Plastic Instability or Limit Load - The failure event is characterized by large deflections and plastic strains associated with ultimate strength collapse.

A diagram showing the relationship between critical and failure stress and flaw size for the three failure modes is shown in Figure 2-1. The shape and position of the failure locus will depend on the fracture toughness (K_{Ic}) and strength properties (σ_y and σ_{uts}) of the material, as well as the structural geometry (t) and type of loading. LEFM is used most appropriately to describe the behavior of low toughness/high strength materials in which

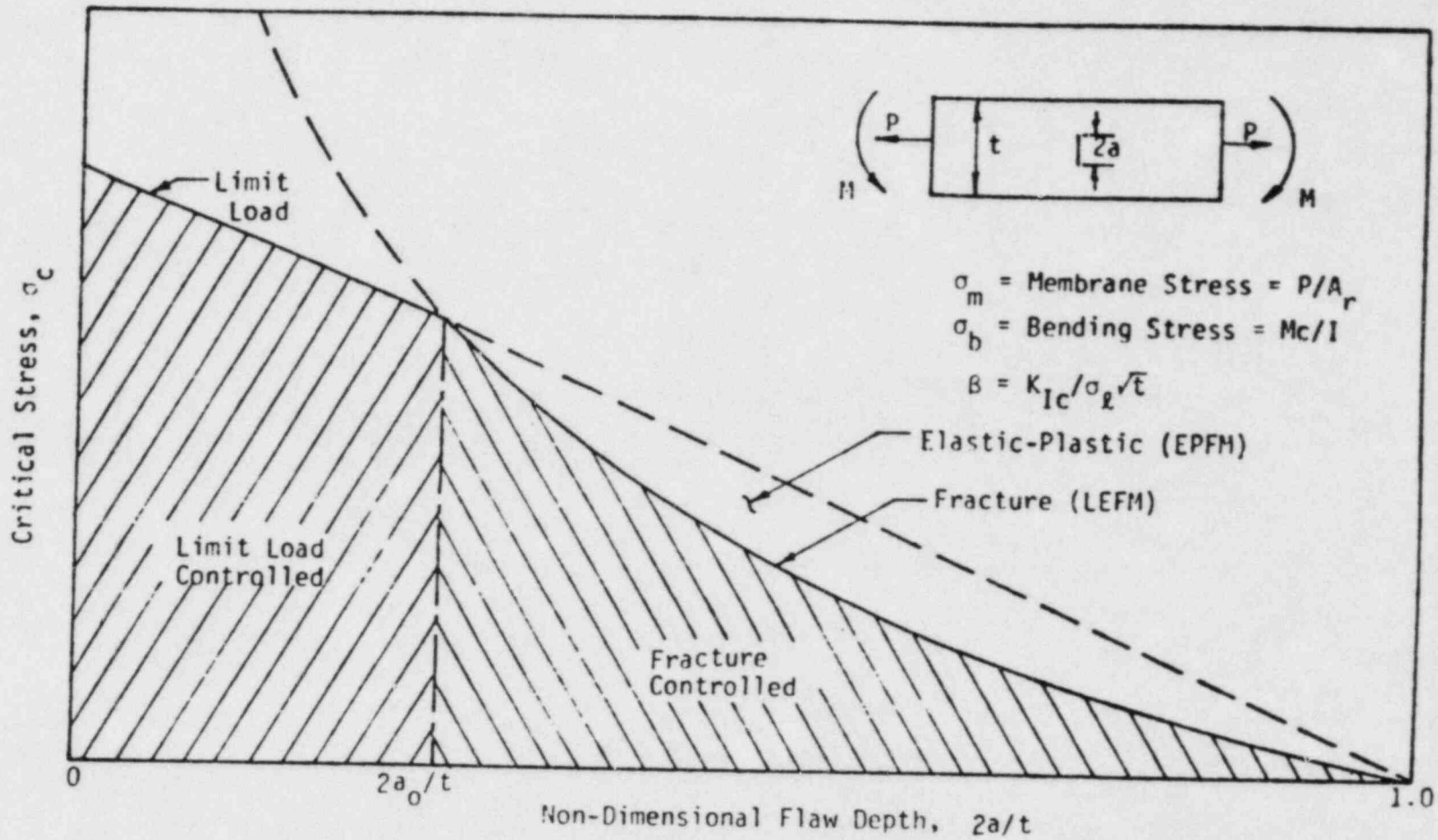

Figure 2-1 - Schematic Showing the Relationship Between Failure Stress and Flaw Size for Two Limiting Failure Modes.

the plastic zone is small relative to the structural geometry and little ductility precedes fracture. With this method, no account is taken of increased material resistance to brittle failure when significant plasticity occurs. Under LEFM conditions, the most useful parameter for characterizing the behavior of cracks is the stress intensity factor, K, which characterizes the singular stresses near the crack tip.

In contrast, plastic instability, when it occurs without prior crack extension, is dominated by the flow properties of the material. In these circumstances, the failure condition is independent of fracture toughness and crack tip characteristics, and a limit load analysis is used to define the failure conditions. EPFM analysis can be used to predict failure behavior in the transitional regime between LEFM and limit load, and under EPFM conditions, the crack tip singularity, the material toughness, and net section strength are all important parameters for failure assessment.

2.2 Failure Behavior of Type 304 Stainless Steel

In deformation studies of Type 304 stainless steel, under monotonic loading, significant ductile behavior has been observed. Specifically, a recent experimental program (2) on the integrity of pipes containing stress corrosion cracks in Type 304 stainless steel pipes has found that:

- "Because of the substantial crack tip blunting that precedes crack growth, the applied stress at failure is virtually independent of the sharpness of the initial flaw introduced into the material."

- "The presence of a weld and any sensitization of the material surrounding the flaw does not significantly affect the applied stress at failure."

- "The exact shape of the flaw is of considerably less importance than the area of the flaw (or of the net flaw area when multiple flaws are present) in determining the applied stress at failure."

The foregoing conclusions are highly supportive of a net-section failure criterion where a limit load analysis will provide a reasonably accurate appraisal of the failure load and the necessary flaw size which could become critical during the service operation of the sparger system. A limit load model is developed in Section 6 to calculate the conditions for final pipe failure.

2.3 Fracture Mechanics Approach to Stress Corrosion Cracking

Structural components containing defects and under combinations of static and alternating loads can experience time-dependent degradation in strength due to subcritical flaw growth. Since crack growth itself may be regarded as damage by determining the extent of crack progression under load, damage can be accumulated and the residual or remining service life can be predicted.

The principles of LEFM effectively link three parameters: the defect size, crack growth rate of the material, and the applied stress, so that if any two of these are known, the third can be quantified. The most useful parameter in describing the character of the near-crack-tip stress distribution is the stress intensity factor. The stress intensity factor, K, defines the magnitude of stress distribution and is calculated in terms of the applied, nominally uniform stress, σ, the crack length, a, and a factor that depends on the flaw geometry, stress distribution, and structural displacement constraints, F(a), from the relation

$$K = \sigma F \sqrt{\pi a}\ , \quad (\sigma < \sigma_y) \qquad (2\text{-}1)$$

Stress corrosion cracking evaluation based on fracture mechanics assumes that flaws are present of size a_i and that the lifetime of a part is that required for a crack to grow from the initial size, a_i, to the critical size, a_f. It has been proposed (3) that crack growth rate data may be correlated to the crack tip stress intensity factor for the given load cycle in the form of relations such as:

$$da/dt = f(K), \qquad (2\text{-}2)$$

where t is a time parameter. By integrating Eq. (2-2) with the appropriate component stress field to calculate K, the time (residual life) for a crack to grow from a_i to a_f is computed from:

$$T = \int_{a_i}^{a_f} \frac{da}{da/dt} \qquad (2\text{-}3)$$

where T is the remaining life in units of time. The final flaw size expected at the end of the design life, a_f, can be determined by Eq. (2-3) with the appropriate stress distribution in the analysis for K by Eq. (2-1) and the desired life T_o from:

$$T_o - \int_{a_i}^{a_f} \frac{da}{da/dt} = 0 \qquad (2\text{-}4)$$

Equation (2-4) is an expression involving a_f that usually must be solved by an iterative process.

2.4 Crack Growth Rate Representation

Many empirical relations to express crack growth behavior have been proposed; the earliest and most well known follows the Paris rule (4) as proposed by Egan and Cipolla (3) which takes a linear form on log-log paper and is represented as

$$da/dt = C K_{max}^{n} \qquad (2\text{-}5)$$

where C and n are constants determined from the data, and K_{max} is the maximum applied stress intensity factor computed from the maximum stress level in the loading cycle. In the remaining life analysis, a more general

rule was used for describing da/dt; specifically, the crack velocity was represented by a piecewise linear curve that best describes the data in a bounding way. This piecewise curve as a function of K_{max} was used in the numerical integration of Eq. (2-4). Section 4 presents the crack growth data used in constructing these curves.

2.5 Development of the Fracture Mechanics Model

A through-thickness crack provides the largest stress intensity factor of the potential models which could have been chosen for this analysis. To provide an upper bound (that is worst case) analysis, this model was used to examine arrest and limit load conditions. This geometry is shown in Figure 2-2. This model was used in both the weld region and away from the weld.

IFI = 201 - CENTER-CRACKED PLATE IN MODE I

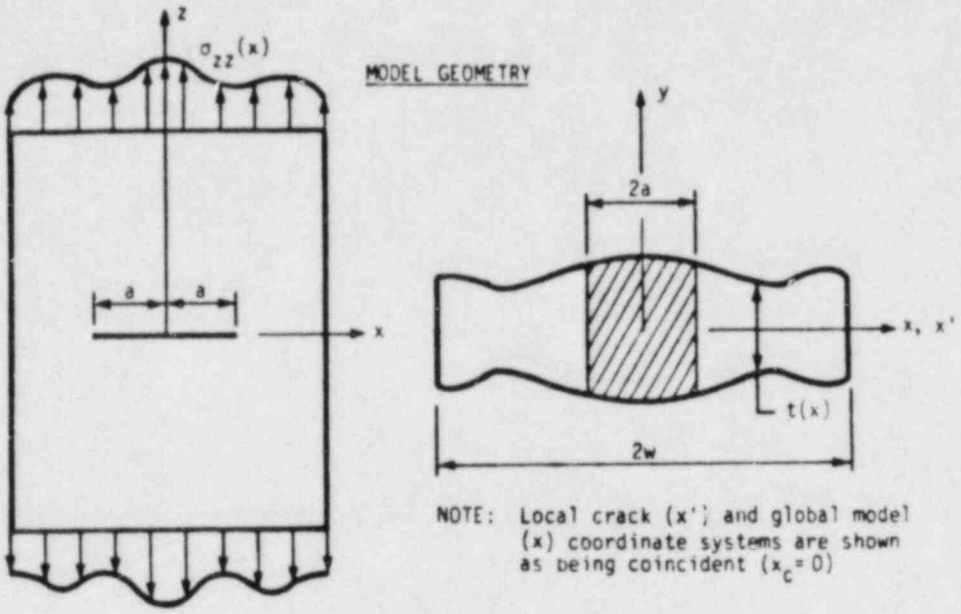

NOTE: Local crack (x') and global model (x) coordinate systems are shown as being coincident ($x_c = 0$)

MODEL DESCRIPTION

MODEL FEATURES	PARAMETER	OPTION FEATURED
Model Index Number	IFI	201
Number of Degrees of Freedom	IDOF	1
Crack Front Shape	--	Straight
Crack Opening Mode	--	Mode I
Finite Width Effects	w	Yes
Variable Thickness Effects	NTH	Yes

Figure 2-2 - Model of Center Cracked Plate (5).

Section 3
ANALYSIS OF STRESS STATE

3.1 Sources of Stress

The sources of stress in the core spray sparger fall into two categories: (1) the residual stress remaining after fabrication, and (2) the actively applied stresses due to service. The residual stresses result from the forming of the pipe bends by rolling, and the subsequent welding together of subassemblies. The service stresses are due in part to heatup/cooldown loads; however, these stresses are small as will be discussed later. The total stress state can affect the analysis in several ways as outlined below:

- The failure mode and cracking mechanism will be affected by stress level
- The magnitude and way in which the stresses are distributed will affect crack arrest considerations
- The magnitude and distribution of stresses will affect crack growth rates
- The magnitude and distribution of stresses will affect final conditions for failure

The different components of stress are discussed next in the remaining subsections. These are the stresses due to rolling fabrication, those due to welding, and finally service-induced stresses.

3.2 Rolling Fabrication Stresses

3.2.1 Analytical Determination

The residual stress state due to rolling is the remaining stress condition resulting from the extent of plastic deformation during the rolling process and the subsequent elastic rebound. An analysis of the stress state in the sparger pipe was performed by General Electric (6) and the result is given here in Figure 3-1. This result was used for preliminary analyses performed except that an account was taken of the actual sparger material properties at operating temperature. As discussed in Section 4, a 550°F yield stress of 23.7 ksi was used to bound the stress distributions. Hence, the stress distributions used in the crack growth analyses assume that the maximum stress level in the stress gradient is limited to 23.7 ksi (the yield strength of the material at 550°F). It should be noted that in the analysis, the origin of cracking was initially taken at the ID location which is in a tensile stress region. However, an additional location on the backside of the pipe was also evaluated since cracks starting from that region, under certain conditions, may become somewhat longer than those located at the ID.

3.2.2 Experimental Measurements

An experimental program was performed by Teledyne Engineering Services, Waltham, Massachusetts, to determine fabrication stresses. The program was performed using curved pipe segments formed on the same equipment used to fabricate the actual sparger. A schematic diagram showing the multi-roll bending procedure is given in Figure 3-2, and the results are shown in Figure 3-3. In Figure 3-3, the measured stresses are plotted along with the theoretical residual stresses calculated by simple beam theory for a curved beam with a circular cross-section.

3.3 Welding Fabrication Stresses

Several major programs (7, 8, 9) have been concerned with the magnitude and distribution of residual stresses in welded stainless steel piping. In

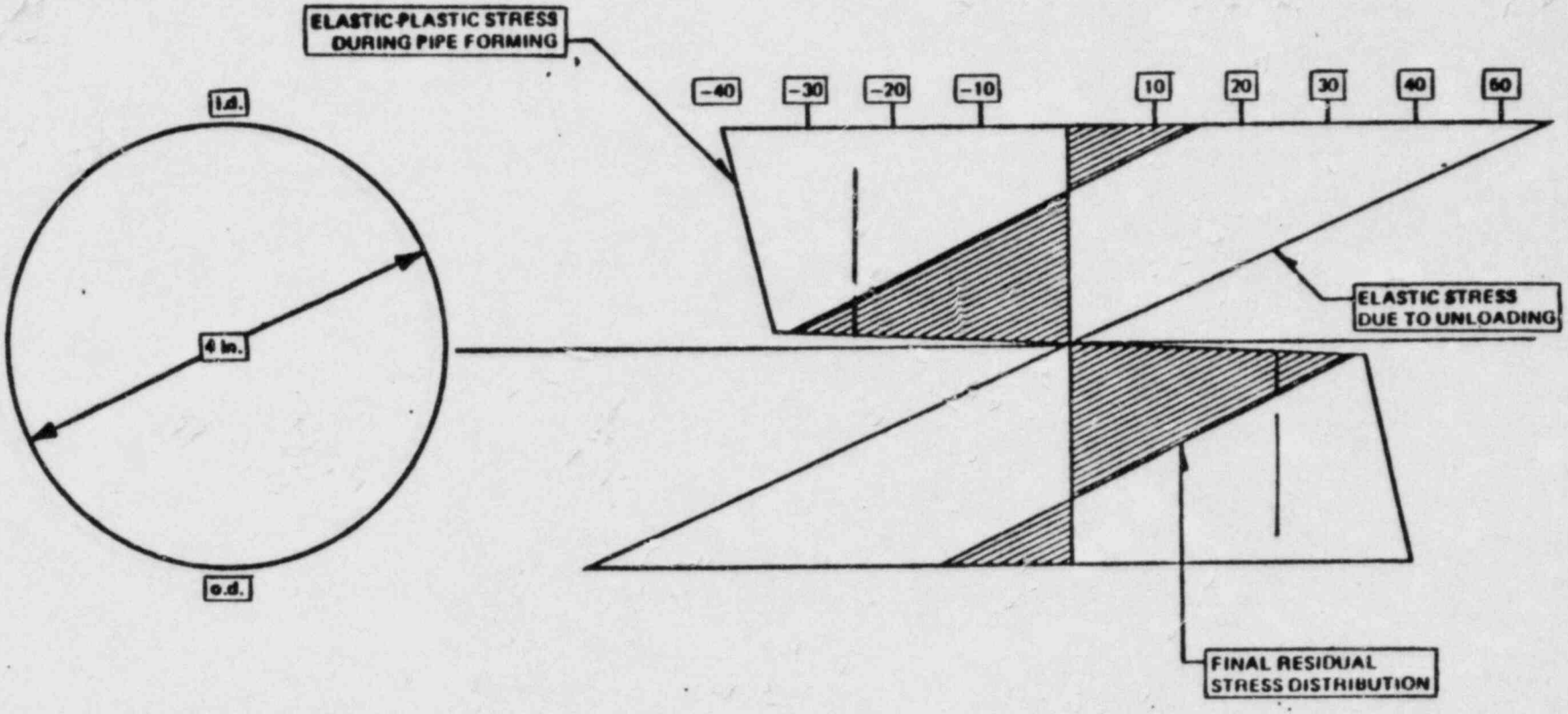

Figure 3-1 - Resultant Residual Stress Distribution After Fabrication (6) and Assumed Relaxation to 550°F Yield (23.7 ksi max).

PILGRIM CORE SPRAY SPARGER PIPE

3-1/2 Inches SCH 40S t = 0.226 Inch

S_y = 37.6 ksi (actual sparger pipe)

S_y = 43.6 ksi (test pipe)

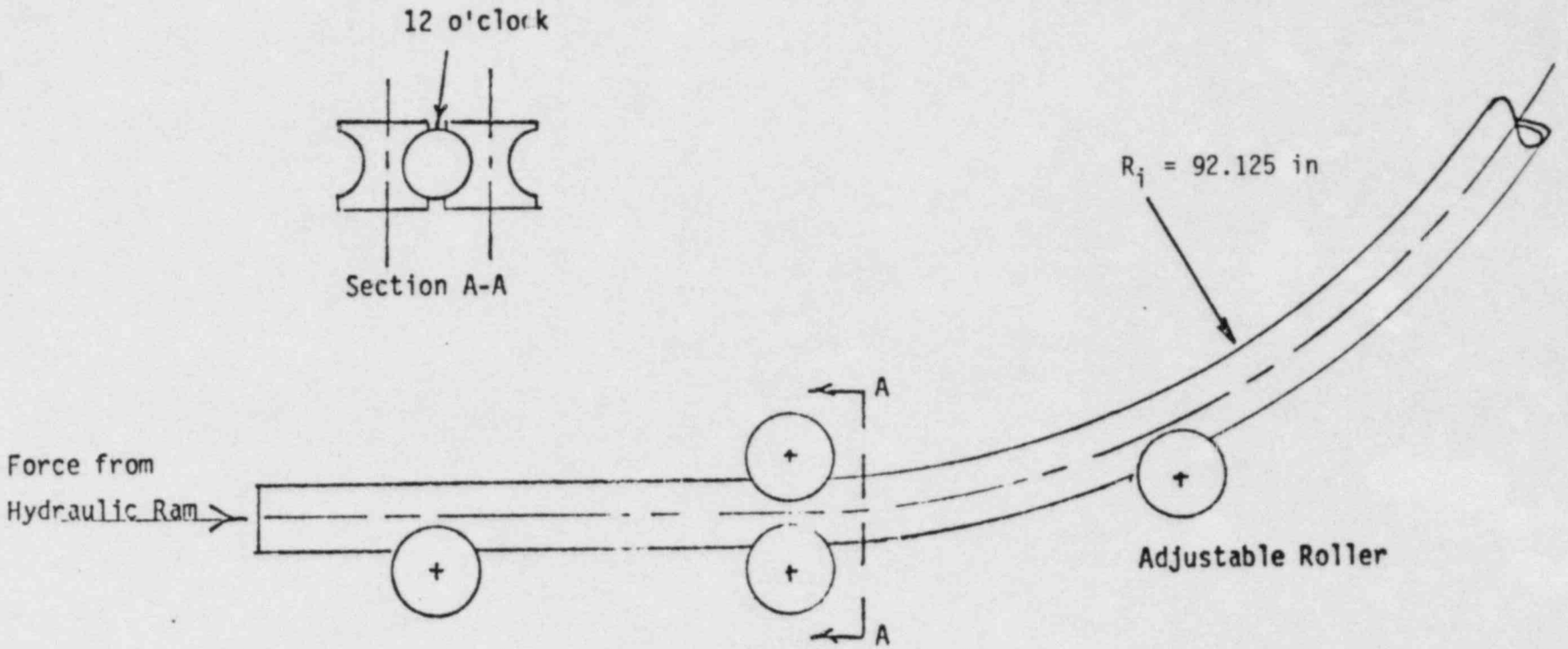

Figure 3-2 - Multi-Roll Pipe Bending Machine.

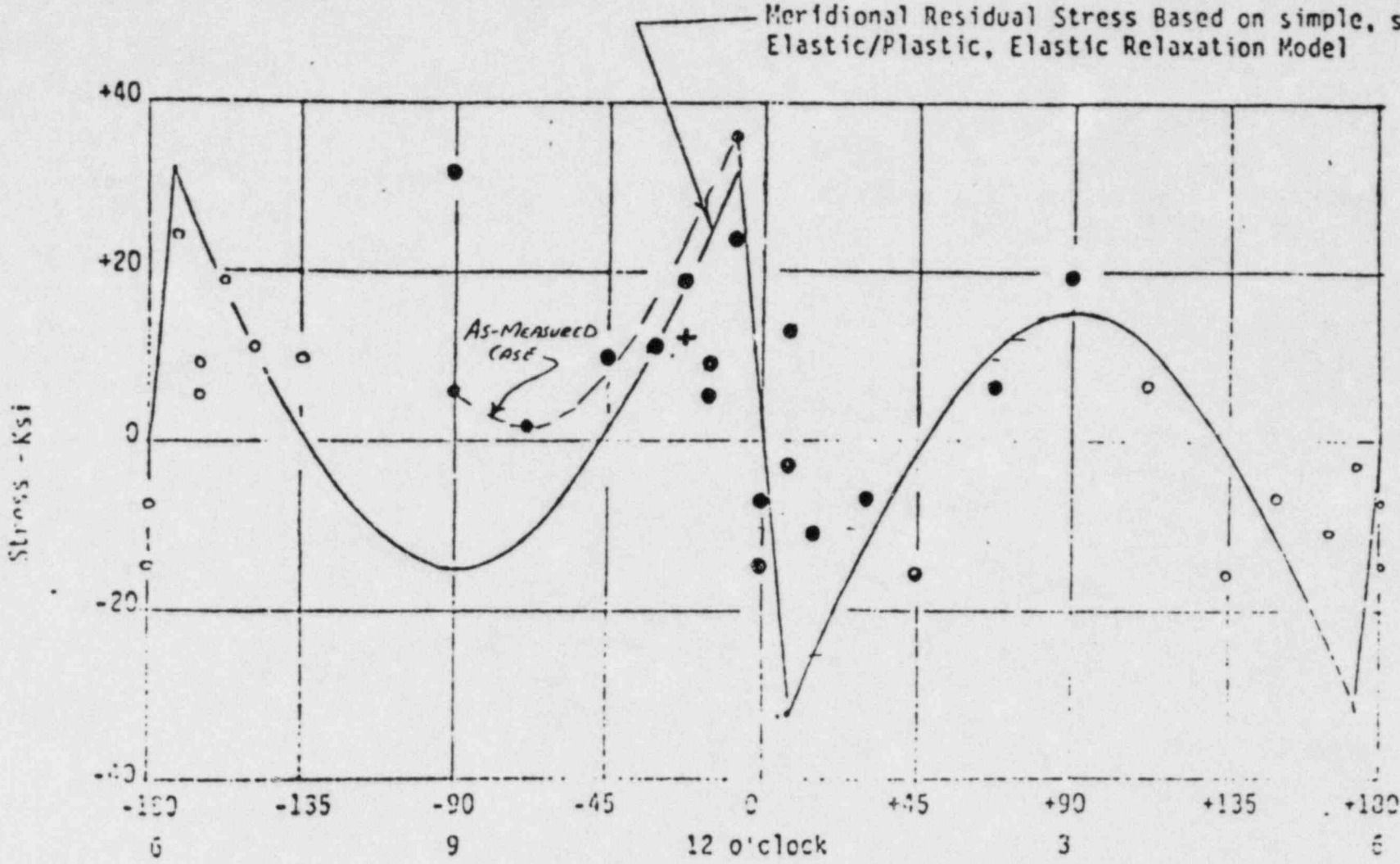

Principal residual stresses (nearer to meridional)

LEGEND (Teledyne Data)

- ● Data points
- o Points based on symmetry
- \+ Single meridional element

Figure 3-3 - Residual Stresses Due to Rolling.

particular, extensive data on butt welds in four-inch diameter lines were obtained as a part of EPRI program RP449-2 (8). The findings of this study, as well as results reported in (10), indicate that yield level tensile residual stresses could exist in four-inch line butt welds. The distribution in stress was non-axisymmetric with a periodic behavior around the pipe circumference. This has several profound influences on crack growth. First, the high tensile stresses can increase the crack growth rate. Second, since residual stresses are self-equilibrating, an axisymmetric distribution will assure that compressive stresses exist at each circumferential location at a through-wall position to balance the tensile surface stresses and thus tend to slow and possibly arrest cracks growing through the pipe wall. For an asymmetric distribution, this assurance is not present. In particular, for the highly asymmetric four-inch lines, through-wall distributions which are completely tensile are observed. Thus, it is not generally possible to arrest surface cracks before they become through-wall.

On the other hand, to balance the tensile regions, there are extensive compressive fields which can act to arrest a through-wall crack as it grows around the pipe circumference. The competing mechanisms of through-wall tensile fields and circumferential compressive locations represent the crack driving force that will determine arrest of a growing crack.

The distribution chosen for this region was that developed for butt welds in four-inch pipes as shown in Figure 3-4. The maximum stress of 23.7 ksi is allowed.

3.4 Service Stresses

The service stresses were found to be small. From (6), "all identified stresses were found to be negligible." Loadings that were considered include impingement loads (i.e., flow past the spargers), seismic loadings, pressure, thermal mismatch, stagnant line top-to-bottom temperature gradients, stagnant line through-wall temperature gradients and weight." These stresses are presented in Table 3-1 taken from (6).

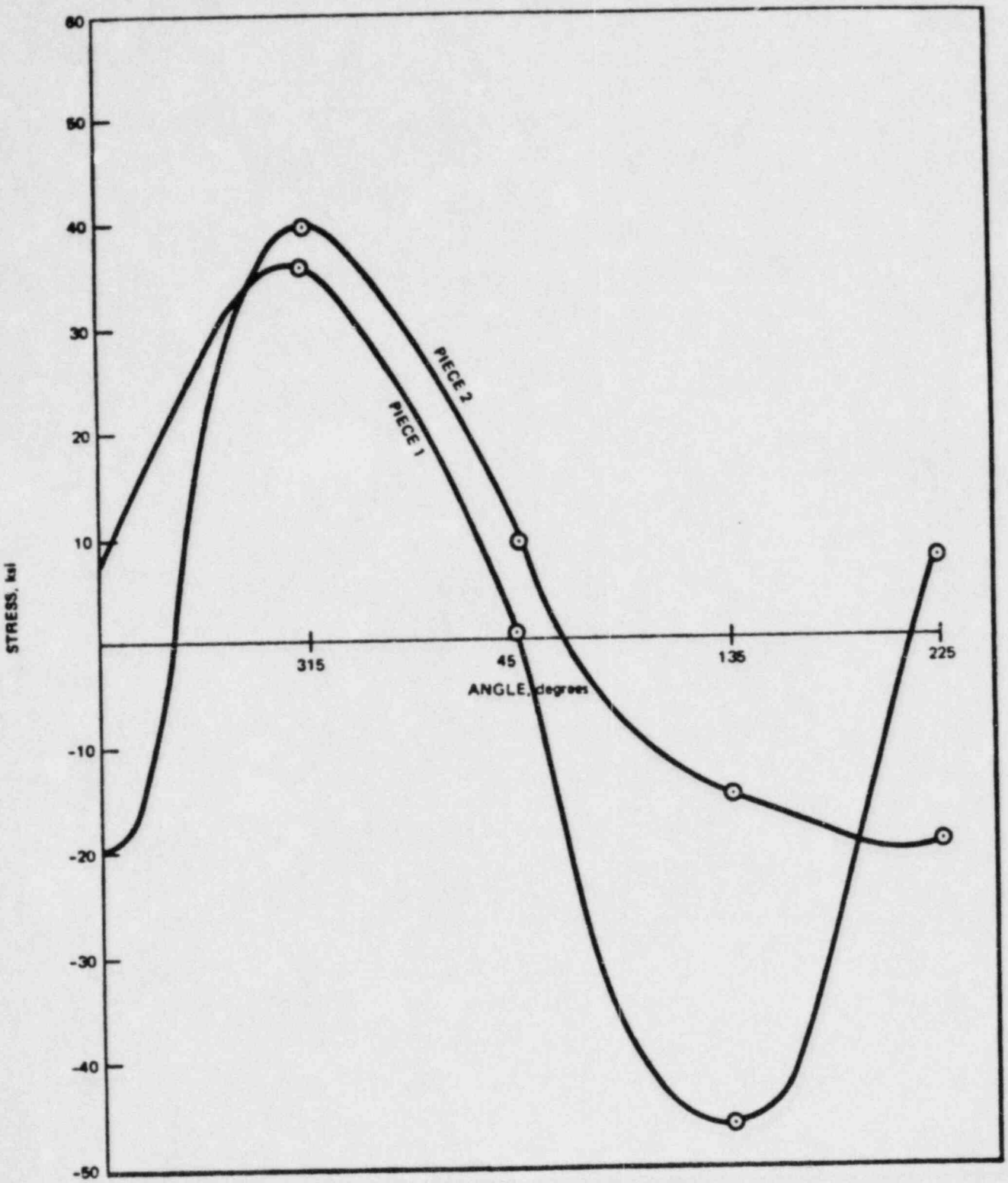

Figure 3-4 - Maximum Surface Residual Stresses For a Four-Inch Pipe Inside Surface at 0.1 Inch From Edge of Fillet of Pieces 1 and 2 Versus Azimuth (10).

Table 3-1

Core Spray Sparger Stress Summary

Load Condition	Assumed Stress Type	Location	Magnitude (psi)
Design:			
Impingement	P_b	pipe at bracket	106 to 509(1)
Seismic (DBE)	P_b	pipe at bracket	283 to 1352 (1)
Pressure (Δp=16psi)	P_m	-	300(3)
Thermal	Q	pipe at bracket	4411
Water Hammer	P_m	-	Negligible(2)
Normal Plant Operation			
Impingement	P_b	pipe at bracket	106 to 509(1)
Seismic (OBE)	P_b	pipe at bracket	236
Cold Spring	Q	bracket or junction box	None
Pressure (Δp=0)	P_m	-	0
Thermal	Q	-	Negligible

(1) The higher magnitude was determined under the assumption that a break (360° crack) exists in the sparger pipe.

(2) Pressure increase due to water hammer is negligible as estimated by GE.

(3) Axial stress due to pressure conservatively includes bracket friction effects as determined by GE (6).

The service stresses are predominately bending in nature, and are derived mostly be secondary type loads. For design conditions, the summary of stress by type of load is given below:

	Primary	Secondary	Total
Tension	300 psi	0	300 psi
Bending	389-1861 psi	4411 psi	4800-6272 psi
Total	689-2161 psi	4411 psi	5100-6572 psi

The design conditions include postulated Emergency Core Cooling Systems (ECCS) loadings that are considered in this report as the short-term loads under which the sparger must safely function for one occurrence. Based on the above summary, the maximum total service stress is approximately 5 ksi but could be 6.6 ksi if a sparger pipe is completely severed at one junction box. Secondary stresses will tend to relax upon crack propagation, therefore, the maximum design stress for limit load considerations of a partially cracked sparger pipe would be approximately 700 psi.

The normal operating loads are long-term service conditions under which a potential for SCC will exist. These stresses are very low and are all primary bending. The absolute stress magnitude is 342 to 745 psi. Since the sparger pipe was fabricated outside the vessel, then lowered into the vessel as a complete unit, no installation stresses caused by cold spring are believed to exist. Hence, only the residual stresses due to pipe rolling and welding provide the driving forces for SCC.

Since it was felt that some questions may arise on the magnitude of the long-term service stresses, a parametric study that includes different levels of applied stress in addition to the residual stress was performed. Specifically, applied axial stress levels of 5 ksi, 10 ksi, and 15 ksi tension and 5 ksi bending were studied. In the analysis, the service stresses were conservatively added to the residual stress state by simple elastic superposition while maintaining the condition of maximum applied

stress limit of 23.7 ksi (approximate yield strength at 550°F). These stress distributions were then used as input into the fracture mechanics analysis for predicting the remaining life of the sparger pipe and the conditions under which crack arrest would occur.

Section 4
MATERIAL PROPERTIES

4.1 Crack Growth Rates

A major factor in assessing the potential for fracture of the core spray sparger during its design lifetime is the rate at which SCC growth can occur. This mechanism is of most interest since preliminary work (6) has shown an absence of fatigue loading, and past work on the SCC of Type 304 stainless steel (10, 11, 12) has shown a susceptibility to this failure mechanism.

The use of crack growth rate information is two-fold. First, if crack arrest cannot be demonstrated, it is often possible to demonstrate analytical lifetimes far in excess of design life, depending on the assumptions for residual stress and the state of applied stress. Second, where such information is available from field observations, it can serve as a check on assumption about applied stresses. Where known crack growth patterns have occurred, it is possible from final flaw dimensions to verify the proposed stress state.

Several major programs have been recently completed or are currently underway (13, 14, 15) to assess the potential growth rate for SCC in Type 304 stainless. Figure 4-1 shows typical data associated with a range of conditions which have been tested in assessing SCC in Type 304. These include various metallurgical structures and environments: furnace sensitized, weld sensitized, annealed and low temperature sensitized, and oxygen content ranging from 0.2 ppm to 8 ppm. Various specimen configurations were also tested to include constant load and constant K loading geometries. Given the scatter in data, it is necessary to pick those data that are most appropriate for a given pipe region, geometry, stress level and environment.

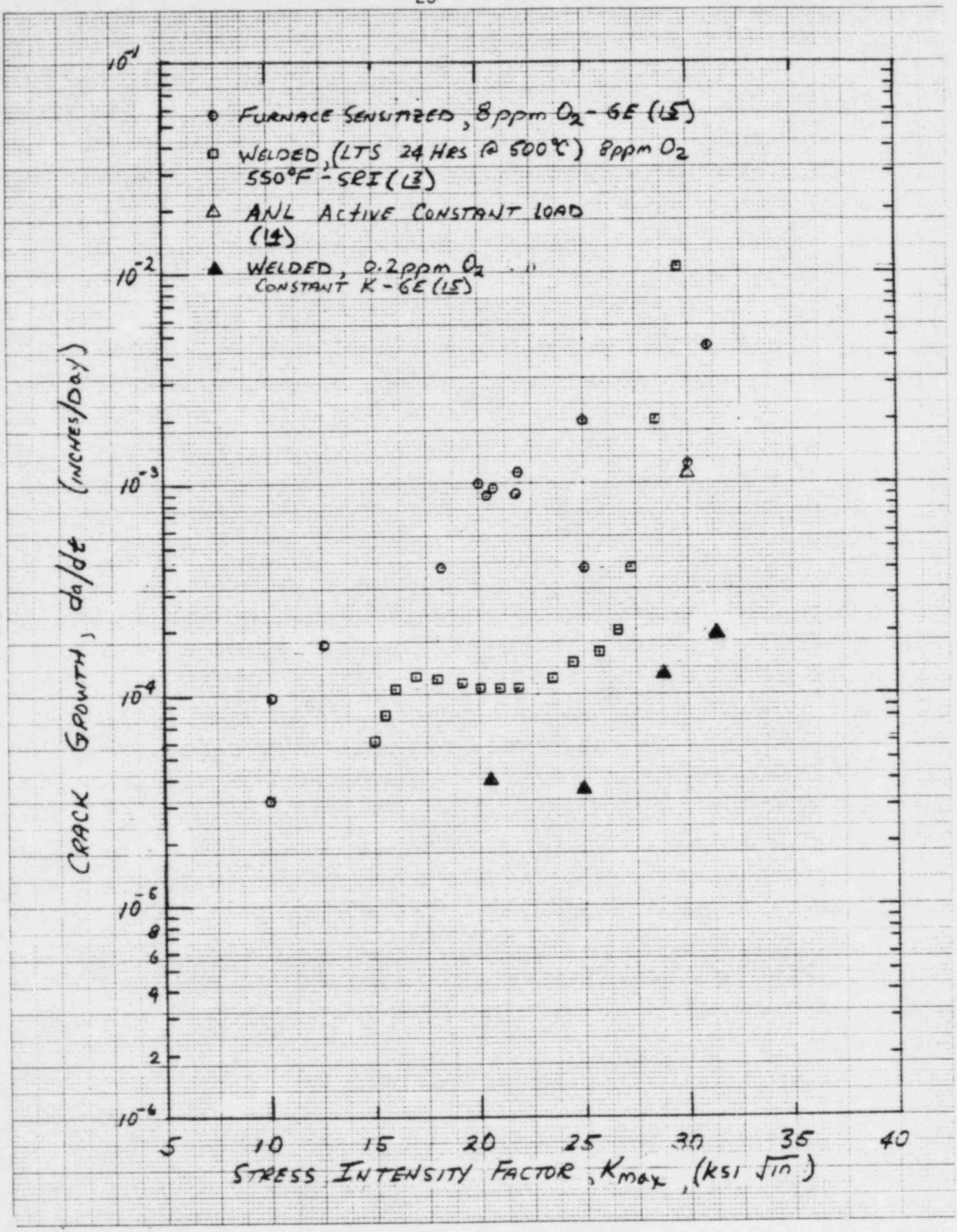

Figure 4-1 - Crack Velocity as a Function of K_{max}.

As has been discussed, the fracture mechanics assessment has examined two distinct regions: (1) those subject to fabrication stresses due to bending, and (2) those subject to subsequent welding residual stresses. Since the data in Figure 4-1 do not represent exactly the conditions that exist at these two locations, two da/dt curves were proposed: one to represent an upper bound (worst case) behavior, and another to provide a more reasonable "best estimate" for crack growth. These two curves are shown in Figure 4-2. Both curves were used in the analysis for remaining life in order to bound the expected service life. A discussion of the use of these curves with relation to the two sparger pipe locations follows next.

4.2 Mid-Sparger Growth Rate

The pipe away from welds has seen the following history. The mill-annealed pipe was bent to shape (see Section 3.1 for details). It was then installed and has been subjected to approximately 5.5×10^4 hours of 550°F exposure in a BWR environment. The fabrication process introduced residual stresses as well as certain metallurgical changes due to cold work. The effect of cold work on the susceptibility of Type 304 stainless has been the subject of a limited amount of work (16, 17). The recent paper by Pednekar and Smialowska (17) provides insight as to its effects. They establish that cold work increases the dislocation density along slip planes and leads to formation of martensitic platelets. Further, with increasingly larger amounts of prior cold work (maximum at 10%), subsequent sensitization treatment results in progressively greater precipitation of carbides, first along the grain boundaries, then within the grains proper. They conclude that: "Small amounts of cold work, as little as 5%, followed by sensitization, can result in extreme SCC susceptibility in Type 304 steel." With these comments in mind, it is possible to establish the following scenario for material condition in the sparger. The mill annealing process performed on the pipe product may not have been sufficient to prevent carbide formation. The subsequent cold rolling increased dislocation density along slip planes and lead to the formation of martensitic platelets, thus, a condition susceptible to crack growth by SCC was achieved. Additional

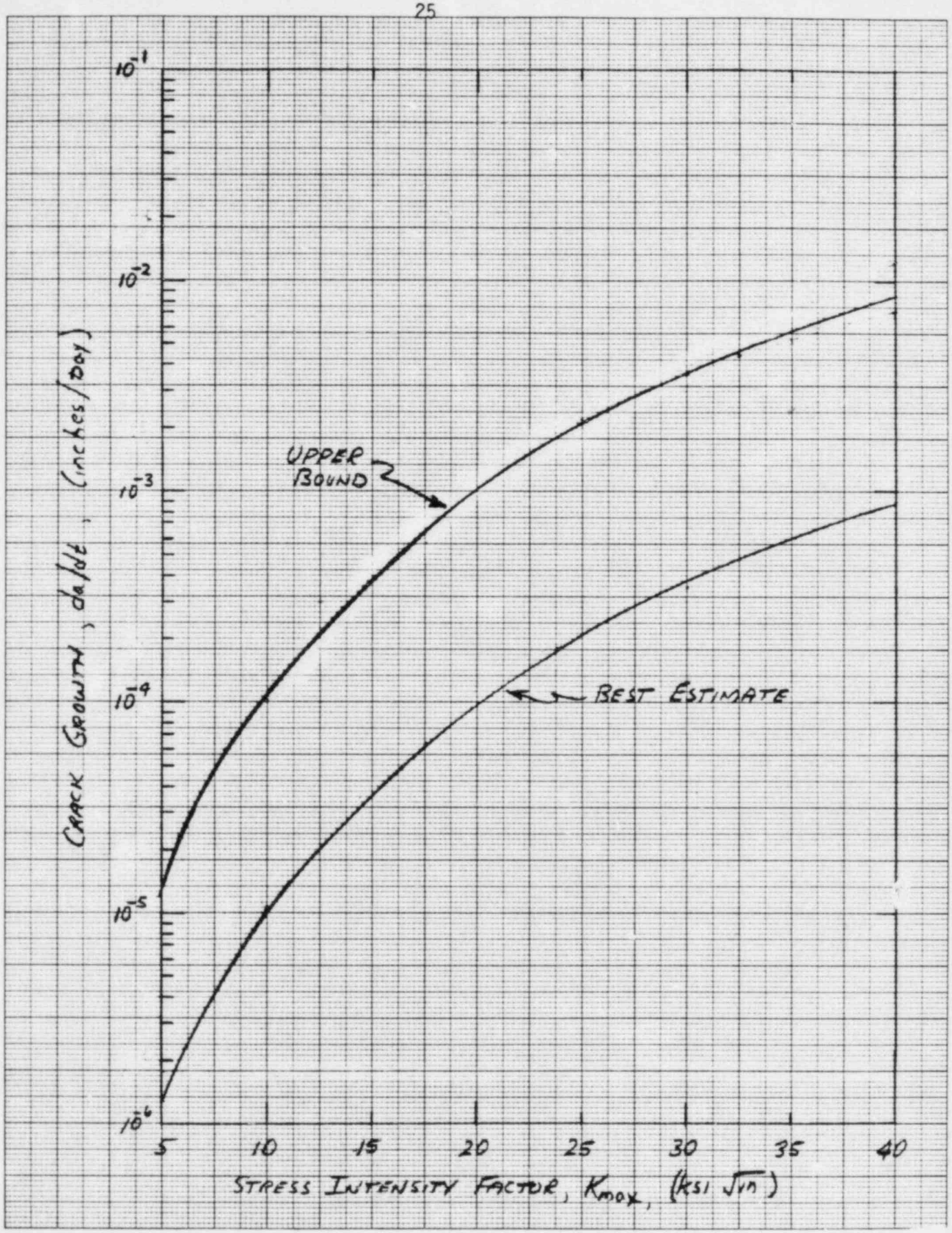

Figure 4-2 - Assumed Crack Velocity Behavior.

sensitization caused by 5.5×10^4 hours of exposure at 550°F could only aggrevate the existing condition.

To provide an upper bound for this analysis, the growth rate associated with furnace sensitized material (15) has been chosen for the analysis. These data were isolated in a curve that represents the behavior as shown in Figure 4-2.

4.3 Near Weld Material Condition

The condition of the material near welds is better characterized, due to the bulk of research which has been directed toward weld sensitization in the last few years. The furnace sensitized growth rates are again used as an upper bound since furnace sensitized material is clearly more susceptible than materials subjected to weld sensitization. It is expected though that the "best estimate" curve in Figure 4-2 is still a reasonable approximation of the material behavior near the fabrication welds.

4.4 Yield Strength

The room temperature yield was reported to be 37,615 psi and the corresponding ultimate tensile strength is 83,660 psi (18). Given a factor of 0.63 for Type 304 on 550°F yield strength to 75°F yield (19), a yield strength of 23.7 ksi has been taken as the 550°F yield strength to bound the stress distributions employed. A comparison with other nuclear grade heats of Type 304 (20, 10) in Table 4-1 shows the chemistry and yield strength of the core spray sparger material is consistent with other piping products. It should be noted that the carbon content of 0.048% is on the low side, making the material less susceptible to weld sensitization and, hence, less susceptible to IGSCC.

Table 4-1

COMPARISON OF SPARGER PIPE HEAT WITH OTHER TYPICAL HEATS OF TYPE 304

HEAT NUMBER	SUPPLIER	C	Mn	Ni	Cr	Mo	σ_y (ksi)
M0063	---	0.050	1.72	10.46	18.64		38.9
M7616	---	0.060	1.72	10.92	18.83		45.8
M7772	---	0.050	1.80	10.15	18.81	0.11	41.1
454659	---	0.045	1.25	9.76	18.40	0.23	35.4
TH6656	---	0.060	1.72	9.30	18.31	0.24	37.0
78500	---						
2P6396	---	0.040	1.65	10.30	18.66	0.20	38.4
834264	---	0.060	1.58	9.12	18.30	0.30	38.5
2P6424	---	0.040	1.65	9.61	18.37	0.25	39.0
454970	---	0.042	1.09	10.10	18.10		37.6
C-15056	Curtiss-Wright	0.040	1.20	9.86	19.82		46.7
C-1513	Curtiss-Wright	0.065	1.25	10.25	19.85		41.1
J-2500-3*	SWEPCO	0.048	1.24	9.36	18.48	0.00	37.6

*All sparger pipes were supplied in Heat J-2500-3.

Section 5
SUMMARY OF INSPECTION RESULTS

The results of the 1980 video tape enhancement have been provided in AES Report 81-10-83, Revision 1 (1) and subsequent letter reports (21, 22). This section will summarize those data to provide a basis for the subsequent interpretation of the fracture mechanics analysis.

Two general regions of interest were established after review and enhancement of the 1980 video tapes. There were indications associated with welds and indications well removed from weld influences. Those regions that had indications associated with weld details, included several that were found not to be cracks, based on work performed during and subsequent to the 1981 inspection. The weld regions which did have indications that could be interpreted as cracks were the B sparger junction box (Figures A-10 through A-19 of (1)) and possibly the A sparger junction box area (Figures A-27 and A.28 of (1)). For these indications, an upper bound length of 3.5 inches was assumed in the analysis. The crack was conservatively assumed to be through the wall of the sparger. This will provide a "worst-case" effect of the crack on structural integrity.

In the other general region, away from welds (also called mid-sparger), the indication of interest was originally considered to be a significant indication but during the 1981 inspection was judged not to be a crack. The area of interest was on the 270° side of the A sparger junction box (Figures A-29 through A-32 of (1)). Despite the finding that this indication was not a crack, the full potential impact on structural integrity was assessed by assuming a crack-like defect equal to the indication length. This will obviously result in a very conservative estimate of the potential for failure in this region.

Section 6
LIMIT LOAD ANALYSIS

6.1 Limit Load Model

The structural integrity of the sparger pipe was assessed with the principles of limit load theory. The criteria for failure is that condition that causes the net or remaining section of the pipe to become fully plastic. The load required to form a plastic hinge in a thin-walled pipe with a through-wall crack was determined analytically for the geometry shown in Figure 6-1. The stress strain behavior of the pipe material is assumed to behave as a rigid perfectly-plastic material. To accommodate for strain hardening, the limit stress (σ_ℓ) for the material is assumed as the average flow stress:

$$\sigma_\ell = (\sigma_y + \sigma_u)/2 \qquad (6\text{-}1)$$

For the values tabulated as specified minimums at 550°F for σ_y and σ_u in the ASME Code (23), σ_ℓ is approximately 45.0 ksi.

The development follows that for a surface flaw where the shift in the neutral bending axis, caused by both the presence of the crack and combined tension-bending, is calculated from a relationship which satisfies force equilibrium in the longitudinal direction given below as:

$$\psi = \frac{[\pi - \alpha(a/t)]}{2} - \frac{\pi}{2}\,\frac{\sigma_m}{\sigma_\ell} \qquad (6\text{-}2)$$

where σ_m is the applied axial stress for the uncracked section and α is the crack half angle. The requirement of moment equilibrium is satisfied through

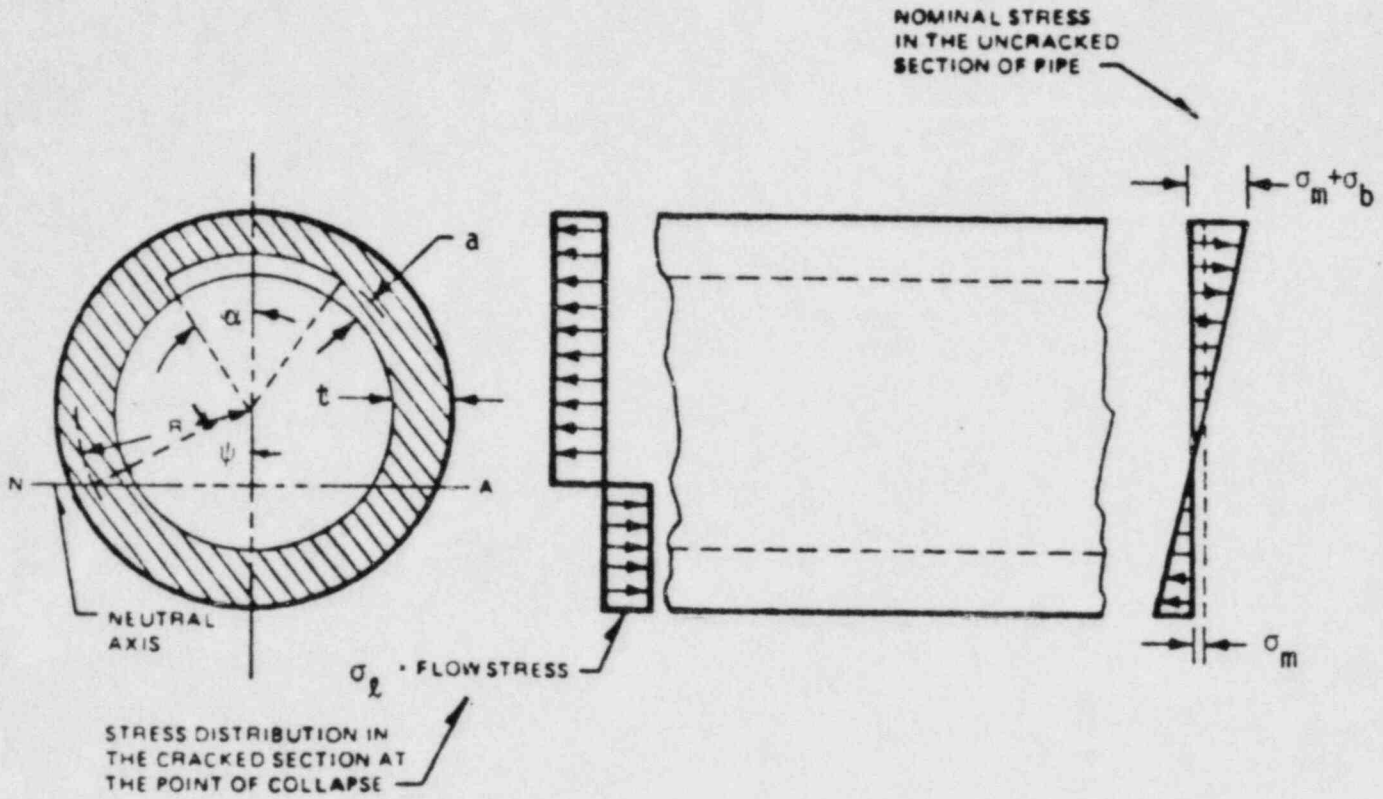

Figure 6-1 - Limit Load Model and Geometry.

integration of the stress distribution across the section and equating with the applied bending moment to give:

$$\frac{\sigma_b}{\sigma_\ell} = \frac{2}{\pi} \left(2 \sin \psi - \frac{a}{t} \sin \alpha\right) \qquad (6\text{-}3)$$

The simultaneous solution of Eq. (6-2) with Eq. (6-3) defines the failure locus for plastic collapse of the section. Since in the derivation of these expressions an assumption was made which idealizes the sparger as a thin-wall cylinder, the location of the flaw relative to the wall thickness (i.e., surface versus subsurface), is not a variable in the solution and the above expressions could be applied to subsurface flaws when 2a/t is substituted for a/t in Eq. (6-2) and Eq. (6-3).

6.2 Numerical Results

In all limit load calculations, only parametric service stresses are utilized. The reason is that the secondary weld residual and service stresses are displacement controlled and will tend to relax during crack growth. The service-induced stresses to be considered in the limit load assessment should therefore be those associated with primary loading. Any inclusion of secondary stress into this analysis will provide for a conservative estimate of critical flaw size. For a crack completely through the thickness of the pipe, the critical crack angle for failure is shown in Figure 6-2. By simple inspection, an applied stress of only 2 ksi will clearly give critical angles much greater than 180°.

For a primary service stress of 300 psi membrane and 389 psi bending determined from design loads calculated by General Electric (6), the critical crack angle for limit load failure is computed as 285° or a crack that is 10.0 inches long. If the sparger pipe is assumed to be severed at one junction box, then limit load failure would be computed for a crack about 258° (or about nine inches long) around the pipe circumference. Hence, very

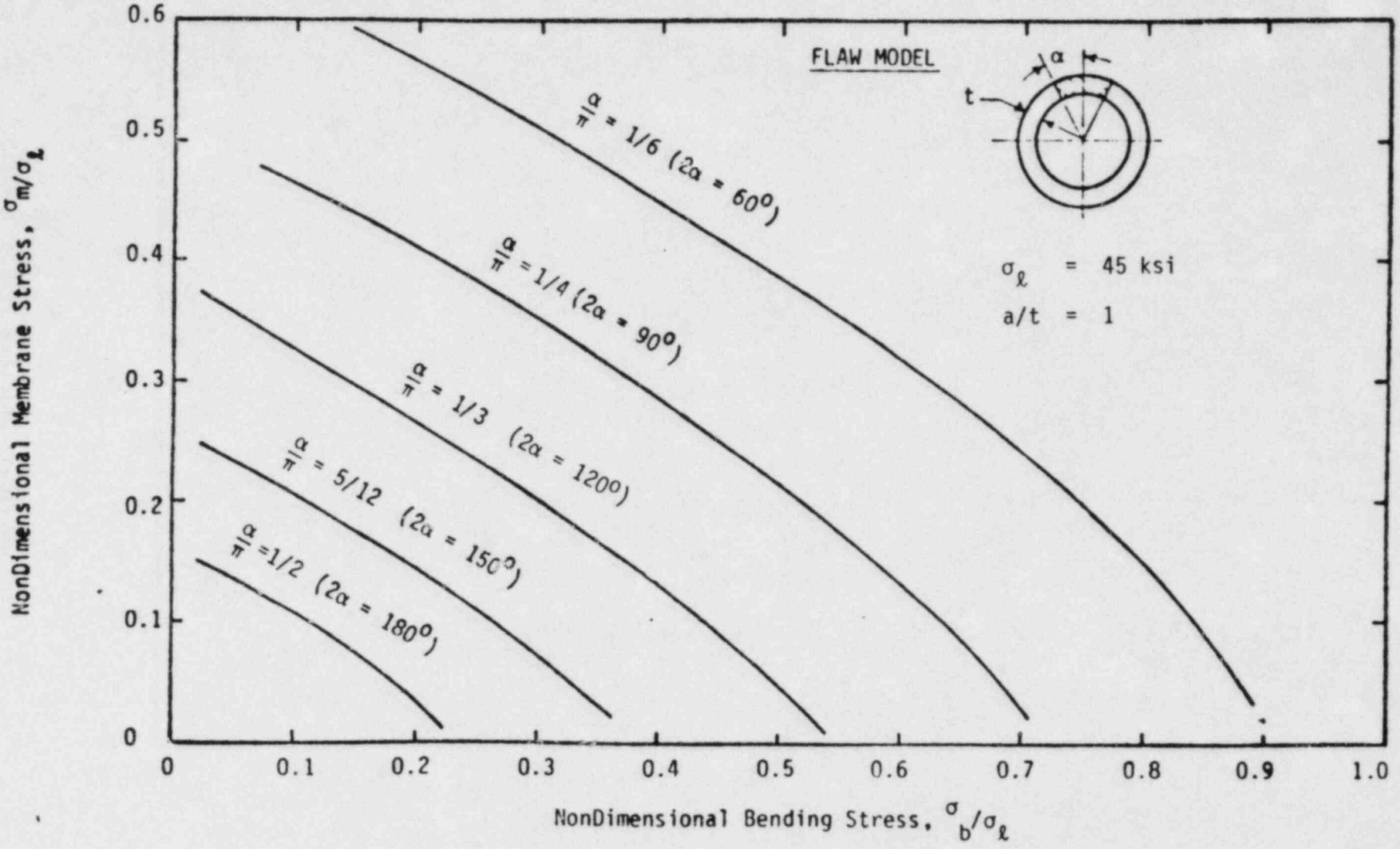

Figure 6-2 - Critical Stress Results For Through-Wall Crack.

long cracks are required to fail by limit load under primary design loads that include seismic, pressure, impingement and water hammer stress events all assumed to occur at the same time. It should be noted that the maintenance action requires an external pipe clamp to be installed when a crack-like indication extends 180° or when the indication extends beyond the inspector's field of view.

Section 7
RESULTS OF STRUCTURAL INTEGRITY AND FRACTURE MECHANICS ANALYSES

7.1 Introduction

This section discusses the calculated results for remaining service life and structural integrity of the core spray sparger pipe. The residual and applied stresses from Section 3 were combined to determine the total stress state. A through-wall flaw was introduced with some small initial length in each of the relevant regions as defined in Section 5. The crack growth behavior was modeled using LEFM techniques as described in Section 2 and using the appropriate crack growth rates of Section 4. Although the long-term service stresses during normal operation are expected to be low as reported in Section 3, the effect of service stress on crack growth was studied parametrically. It is anticipated that the results presented herein will be used to predict expected flaw sizes given the current state of the sparger as determined by periodic inspections.

Flaws were modeled as growing by a stress corrosion mechanism to one of three final states. These are:

- A length such that the flaw exceeded the limit length calculated as described in Section 6
- The crack arrested owing to the distribution and characteristics of the stress state
- The expected lifetime to State 1 or 2 exceeded the plant design lifetime

The two regions of interest, one away from any sparger pipe weldments and the other near the pipe welds are discussed separately. A third region was also addressed. This was away from the weld but on the "back" side (not inspectable) of the sparger. This analysis was performed for the sparger pipe region away from any weldments. At each region, a through-wall circumferential crack was postulated at the intrados or core-side surface of the sparger pipe. The crack length as a function of time was computed by integrating Eq. (2-3). Crack arrest is predicted when the stress intensity factor becomes zero, and the flaw lengths when this occurs are indicated in the results.

7.2 Region Away From Welds

The long indication observed near Junction Box A but away from any welds (mid-sparger) was determined not to be a crack. However, as a bound, this region was evaluated assuming a postulated through-wall crack, and the crack growth as a function of time was calculated for a range of applied stress levels. These results showing the corresponding effects of stress level and material crack growth rate on calculated flaw lengths, are plotted in Figure 7-1. This figure gives flaw length as a function of time for five states of stress: the theoretical residual stress state only as well as several cases of the residual stress plus parametric service load cases. The service loads were taken at levels of 5, 10, and 15 ksi membrane and 5 ksi bending stresses. The calculated arrest lengths are shown for all cases, except residual stress plus 15 ksi membrane stress which will not arrest. For all other cases, arrest will occur before critical size for that stress level is reached as calculated from net section failure criteria.

The expected crack extension for an 18-month period was determined from the results in Figure 7-1. For a given observed flaw size, the flaw size that would be observed after 18 months of additional service is shown in Figure 7-2. These results are based on the upper bound crack growth behavior and can be used to predict conservatively the amount of crack growth between refueling outages if the time span between inspections is 18 months or less.

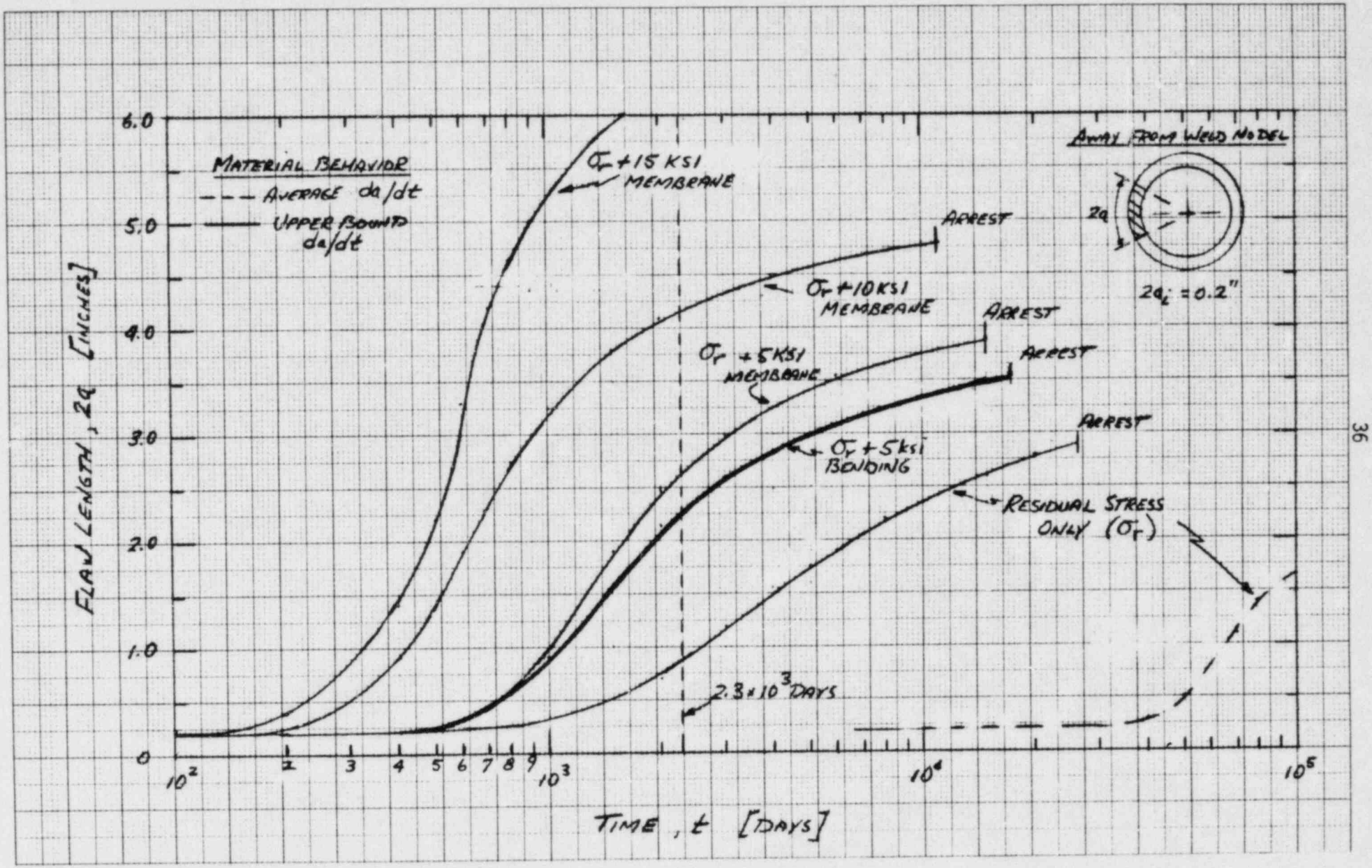

Figure 7-1 - Effect of Stress Level and Material Crack Growth Rate on Flaw Length vs. Time For Front-Side Indication Away From Weld Region.

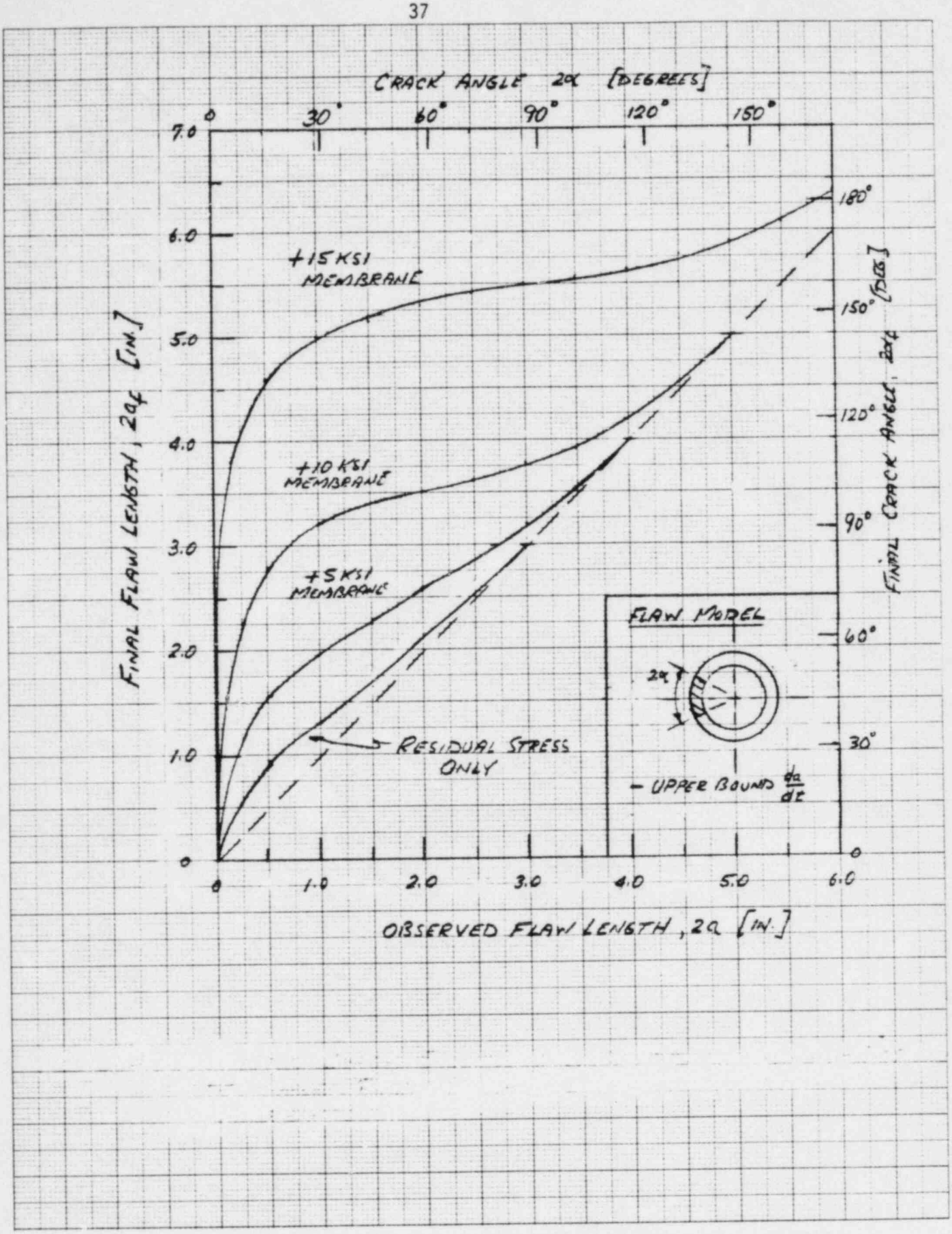

Figure 7-2 - Predicted Crack Growth For Indications on Front-Side of Sparger Pipe Away From Welds For 18 Months of Operation.

For example, an observed flaw length of 3.2 inches would grow to approximately 3.3 inches if the applied stresses in that region are 5 ksi tension. The 10 ksi and 15 ksi applied stress curves would predict a final flaw size of about 3.8 and 5.5 inches, respectively. The point of tangency between the curve and the 45-degree line represents the point where the crack is predicted to arrest.

7.3 Region Near The Weld

A similar analysis was performed for a flaw postulated to exist near a sparger pipe weld connection. The weld residual stress distribution was assumed to have a sinusoidal shape along the pipe circumference having a peak stress of yield strength level and a period equal to the pipe circumference as discussed in Section 3. The results for this analysis are given in Figure 7-3. A comparison of Figure 7-3 with Figure 7-1 indicate that much longer cracks are possible in the regions influenced by the weld. Calculations for the residual stress only case show crack arrest at a final flaw length of about 9.8 inches. Crack lengths greater than 10 inches are possible for the applied stress level as shown in Figure 7-3. Crack arrest for the cases of 5 ksi, 10 ksi, and 15 ksi is still possible if the applied service stresses are secondary in nature. The potential for limit load failure exists if primary stresses are present; however, for the primary stresses specified by General Electric (see Section 3), the critical flaw size for limit load conditions could reach 10 inches or a pipe with a 285° circumferential crack.

The predicted crack growth for an 18-month period based of operation as a function of the length of the observed indications is shown in Figure 7-4. In this figure, both upper bound and mean crack growth rate results are plotted for comparison. The final flaw length is very sensitive to the material behavior and a wide range in crack length can be predicted depending on the crack growth rate assumed. For example, as a best estimate, a flaw of length 3.5 (can grow to approximately 4.4 inches over 18 months, or it can grow to as long as 8.4 inches under worst case material behavior. It is

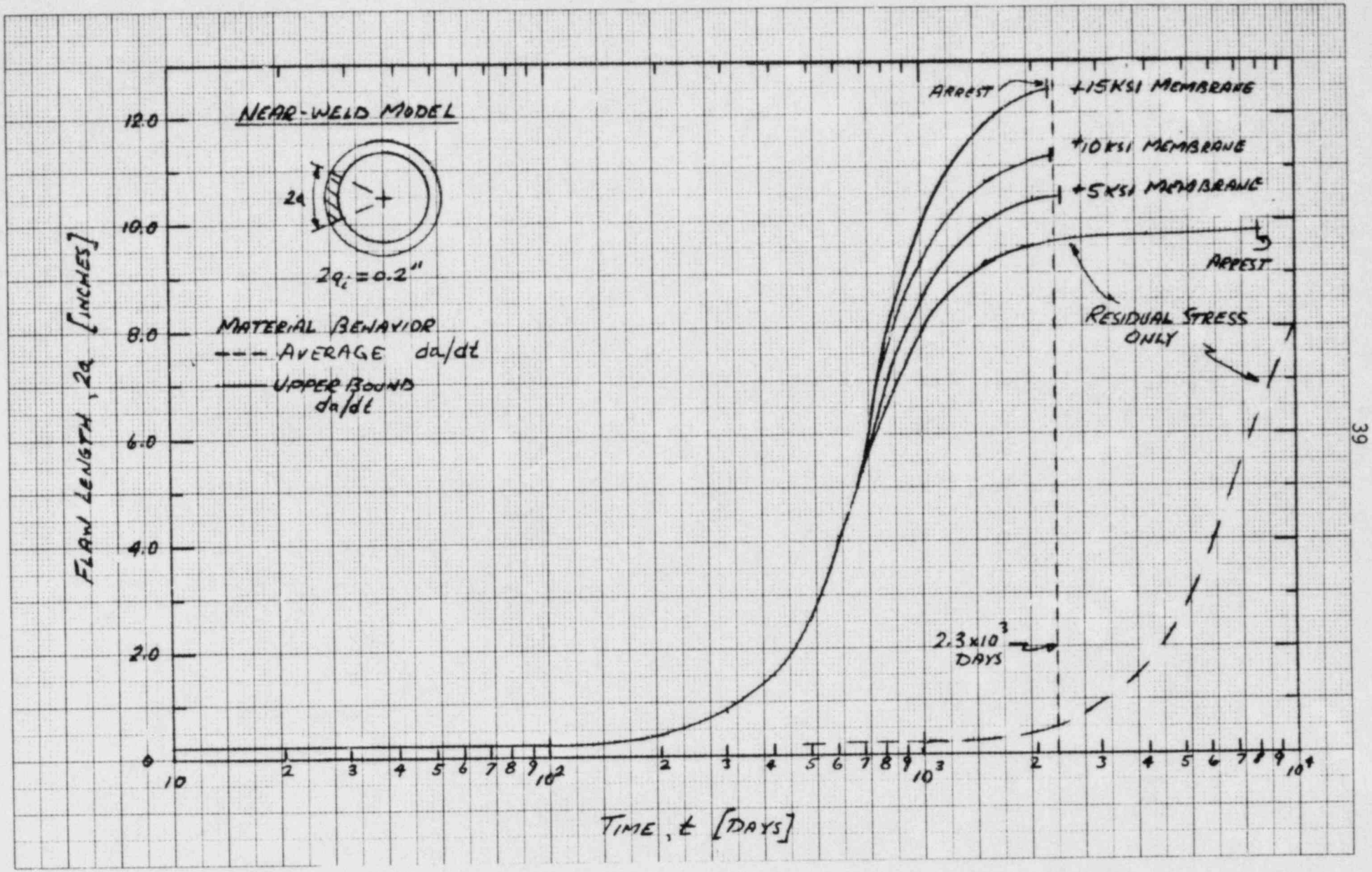

Figure 7-3 - Effect of Stress and Material Crack Growth Rate on Flaw Length vs. Time For Indication Near a Weld.

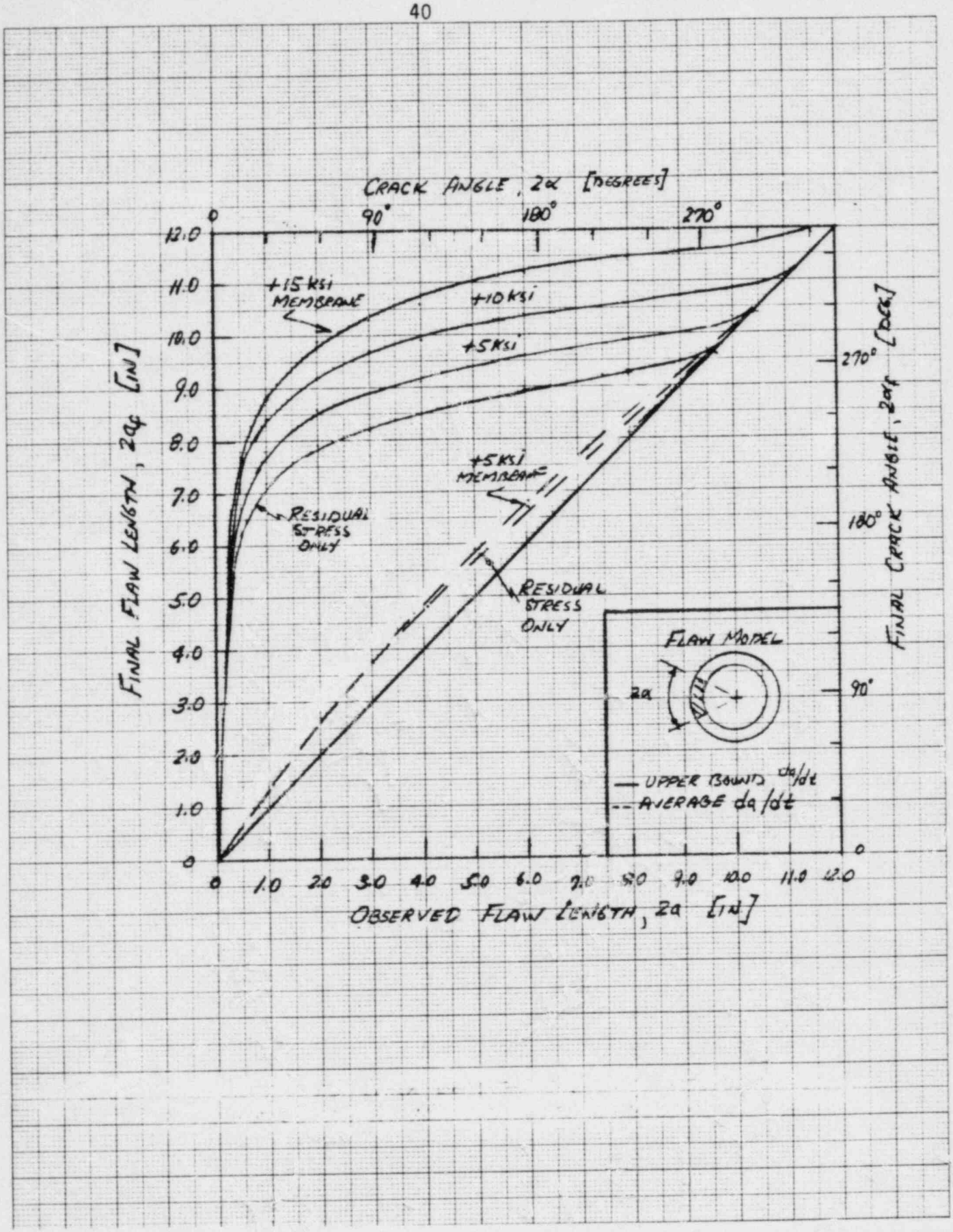

Figure 7-4 - Predicted Crack Growth for Indications Near Welds Over 18 Months of Operation.

important that these predictions be used in conjunction with multiple inspection data gathered over a long period of time. Such comparisons will validate the evaluation method and provide a means of calibrating the model to the field observations. Comparison between the inspections of January 1980 and October 1981 indicates insignificant changes in the observed indications. Clearly, this suggests that the fracture mechanics model and upper bound input data are providing a conservative estimate for the amount of crack extension that could occur.

7.4 Back-Side Defect Evaluation

The potential for flaws to initiate and grow on the back-side of the sparger pipe was evaluated. The results obtained are given in Table 7-1. assuming upper bound crack growth rate behavior. If the measured tensile stresses on back-side (see Figure 3-3) are an indication of a local surface stress effect, then the theoretical stress distribution would be more representative for long flaws. This model predicts crack arrest when the crack is visible (~210°). However, a conservative assessment of the tensile stresses "as measured" on the back-side does not predict crack arrest. It should be noted that the limited test data shown in Figure 3-3 show considerable scatter, particularly on the back-side of the pipe. Because "hand jacking" was used for final pipe curvature adjustments, it is believed that non-uniform and highly localized stresses may exist in the sparger pipe. Table 7-2 gives the remaining time for cracking beyond 180°, at which point the back-side crack just becomes visible from the front side.

TABLE 7-1

SUMMARY OF CRACK GROWTH PREDICTIONS
FOR BACK-SIDE FLAW

CRACK GROWTH 2α	TIME (MONTHS) AS-MEASURED[1] σ_r ONLY	AS-MEASURED[1] σ_r+5Ksi	THEORETICAL σ_r ONLY	THEORETICAL σ_r+5Ksi
7^o to 180^o	1484	160	-[2]	-[2]
180^o to 360^o	1928	37.1	Arrests @ 204^o	Arrests @ 226^o

1 See Figure 3-3 for assumed stress distribution.

2 Theoretical distribution gives negative stress on back-side so cracking will not initiate. If measured tensile surface stresses are local, as expected, the distribution shown in Figure 3-3 will also result in limited crack growth.

FLAW MODEL

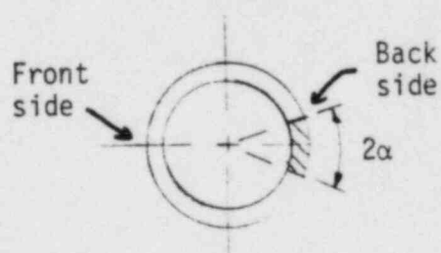

TABLE 7-2

COMPUTED REMAINING TIME FOR A
VISIBLE BACK-SIDE FLAW INDICATION

	REMAINING TIME (MONTHS)			
	AS-MEASURED (1)		THEORETICAL	
CRACK ANGLE 2α	RESIDUAL ONLY	RESIDUAL +5Ksi	RESIDUALS ONLY	RESIDUAL +5Ksi
180^{o}	1928	37.1	112	38.8
183^{o}	1927	36.8	-	-
193^{o}	-	-	3.0	36.8
204^{o}	-	-	0 (Arrest)	-
218^{o}	1913	32.2		-
226^{o}	-	-		0 (Arrest)
259^{o}	1770	22.0		
308^{o}	14.5	6.6		
360^{o}	0 (No Arrest)	0 (No Arrest)		

1 See Figure 3-3 for stress distribution.

FLAW MODEL

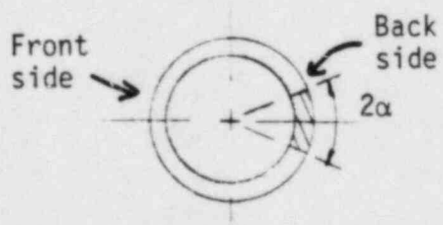

Section 8
SUMMARY AND CONCLUSIONS

- Fracture mechanics analyses have been performed for defects postulated to extend through wall in two general regions of the Pilgrim Station core spray sparger. These regions are away from welds and near welds.

- The following conservatisms were present in this analysis:

  - Upper bound crack growth rates are used

  - Bounding stress fields are used

  - Assumption of through-wall cracks even with regions where indications were determined not to be cracks

- A through-wall crack located away from a weld will arrest given "service" stresses less than 10 ksi membrane tension. Further, this arrest length is shorter than the critical length to cause failure by a net section mechanism under the conservative assumption that the service-induced stress is due to a primary load.

- A through-wall crack located in the region of a weld detail will arrest prior to reaching critical length to failure, given the low applied service stresses as specified by General Electric. Crack growth beyond approximately 10 inches will not assure protection against limit load failure; however, constraint in displacement and rotation may limit the concern for plastic collapse. The length of time required for substantial crack growth in the weld region may also allow a reasonable period from detection to arrest or potential

failure. As a precautionary measure, the maintenance action plan requires the installation of an external pipe clamp when the length of the crack indication is found or predicted to be greater than 180° (6.3 inches).

- The identified indications do not jeopardize structural integrity of the core spray sparger over the next 18 months.

- Crack growth between inspection periods (i.e., 18-month interval) is predicted to be small. For the indication lengths observed away from any welds, crack extension is less than 0.1 inch of growth. Near the sparger pipe weldments, it is predicted that the maximum crack growth will be less than 1 inch.

REFERENCES

1. Hayward, J.A., R.C. Cipolla, and A.J. Sanders, "Computer Enhancement of Video Tapes of ISI of Pilgrim Core Spray Sparger", Phase 1, Preliminary Report, Revision 1, Aptech Engineering Services, AES-81-04-60 (April 1981).

2. "Mechanical Fracture Predictions for Sensitized Stainless Steel Piping With Circumferential Cracks," Final Report, EPRI Research Project RP 585-1, Report NP-192 (June 30, 1976).

3. Egan, G.R. and R.C. Cipolla, "Stress Corrosion Crack Growth and Fracture Predictions for BWR Piping," American Society of Mechanical Engineers, Paper 78-Mat-23 (1979).

4. Paris, P.C., M.P. Gomez and W.D. Anderson, "A Rational Analytical Theory of Fatigue," The Trend in Engineering, Volume 13, No. 1 (January 1961).

5. Besuner, P.M., D.C. Peters, and R.C. Cipolla, "BIGIF: Fracture Mechanics Code for Structures," EPRI Report NP-838 (July 1978).

6. "Supplement 1 to Supplemental Reload Licensing Submittal for Pilgrim Nuclear Power Station Unit 1 Reload 4," General Electric Nuclear Power Systems Division, NEDO-24224-1, Supplement 1 (March 1980) (CD-2).

7. Shack, W.J., W.A. Ellington and L.E. Pahis, "The Measurement of Residual Stress in Type 304 Stainless Steel Piping Butt Weldments," Electric Power Research Institute, Final Report No. RP449-1 (December 1978).

8. Giannuzzi, A.J., "Studies on AISI Type 304 Stainless Steel Piping Weldments for Use in BWR Applications," EPRI NP-944, Research Project 449-2, Final Report.

9. Rybicki, E.F., P.M. McGuire and R.B. Stonesifer, "Effect of Weld Parameters on Residual Stresses in Boiling Water Reactor Piping Systems," EPRI, Semiannual Report RP 1174, April 1, 1978 to October 1, 1978.

10. Kiepfer, H.H., et al., "Investigation of Cause of Cracking in Austenitic Stainless Steel Piping," General Electric Report NEDO-21000, 75-NED35, Class 1 (July 1975).

11. Clarke, W.L. and G.M. Gordon, "Investigation of Stress Corrosion Cracking Susceptibility of Fe-Ni-Cr Alloys in Nuclear Reactor Water Environments," Corrosion, Volume 29, No. 1, pp. 1-12 (January 1973).

12. Park, J.Y., and W.J. Shack, "Corrosion Studies of Nuclear Piping in BWR Environments," Semi-Annual Report for Period ending 31 July 1979, EPRI Research Project 449-1.

13. Caiglurl, R.D., et al., "Low Temperature Sensitization of Weld Heat Affected Zones in Type 304 Stainless Steel," Stanford Research Institute, EPRI Contract T-110-1.

14. Park, J.Y., and W.J. Shack, "Crack Propagation Rate Studies," Argonne National Laboratories, EPRI Contract T117-1.

15. Horn, R.M., et al., "Crack Growth/Arrest Studies," General Electric Company, San Jose, EPRI Contract T118-1.

16. "Basic Studies on the Variables of Fabrication Related Sensitization Phenomena in Stainless Steels," General Electric Company, Schenectady, New YorK, EPRI Research Project RP 1072-1.

17. Pednekar, S. and S. Smialowska, "The Effect of Prior Cold work on the Degree of Sensitization in Type 304 Stainless Steel," Corrosion, 0010-9312/80/000189, p. 565-577.

18. O'Connor, H.W., Trip Report entitled "Core Spray Sparger Visit to Sun Ship Works and Philadelphia Pipe Bending," (April 14, 1981).

19. Peckner, D. and I.M. Bernstein, Handbook of Stainless Steels, McGraw-Hill Book Company, New York (1977).

20. Egan, G.R., R.C. Cipolla and W.P. McNaughton, "Stress Corrosion Cracking Testing Methods Applicability to Plant Performance," AES 81-07-77, Final Report EPRI Project 1562-1.

21. Letter report from Aptech Engineering Services to F.N. Famulari, Manager, Pilgrim Nuclear Power Station, dated October 29, 1981.

22. Letter report from Aptech Engineering Servics to F.N. Famulari, Manager, Pilgrim Nuclear Power Station, dated November 10, 1981.

23. American Society of Mechanical Engineers, Boiler and Pressure Vessel Code, Section III, 1980 Edition.

APPENDIX

PROPOSED PILGRIM CORE SPRAY SPARGER EVALUATION PLAN

APTECH engineering services, inc ENGINEERING CONSULTANTS

795 SAN ANTONIO ROAD • PALO ALTO • CALIFORNIA 94303 (415) 858 • 2863

PROPOSED PILGRIM CORE SPRAY SPARGER EVALUATION PLAN

Areas of Interest

1. Sparger pipe away from weld
2. Sparger pipe to junction box weld HAZ (all welds)
3. Nozzle weld HAZ (all welds)
4. Core spray jumper pipe weld HAZ (all welds)

Strategy for identification of crack indication, crack growth rate, and crack arrest

1. The sparger crack indication identified during the 1980 ISI shall form the basis of reference cracks. Image enhanced photographs taken from video tape records will be used for this purpose.
2. It is essential that reference cracks be established for determining the rate of crack growth. In order to achieve this goal with some degree of confidence and accuracy, approximately 10 reference indications will be identified for thorough examination during the 1981 ISI. Inspection techniques will include the capability to measure crack length and width.
3. Since the quality of the 1981 ISI will be greatly improved and computer image enhancement information will be available, it is expected that the extent of cracking can be quantified within approximately 180^{0} of the exposed surface. Accordingly, previously undetected or recently formed cracking may be found.
4. Comparison of 1981 ISI results to 1980 reference indications will provide improved fracture mechanics evaluation basis for crack growth. The recent work by APTECH will be refined to include these data for crack growth and arrest predictions for fuel cycle 6 (March 1983). Structural integrity evaluations will be modified as necessary.

Maintenance Action Criteria

Maintenance action decisions will be made on a case by case basis and may be dependent upon the ability to reliably predict crack growth rate for fuel cycle 6. In addition, there exists some uncertainty in the nature of residual stresses induced by sparger pipe fabrication and rolling. Therefore, cracking patterns may not be identical in different regions along the pipe. In particular, the condition of the backside of the pipe (extrados), presents some concern due to experimentally measured tensile stresses of varying magnitudes where crack propagation could continue. That area is on the blind side (extrados) and cannot be inspected visually.

Based upon the brief discussion above and analytical and experimental work performed or reviewed by APTECH, the following maintenance criteria are recommended

APTECH ENGINEERING
SERVICES, INC.
795 SAN ANTONIO ROAD
PALO ALTO, CALIFORNIA 94303

to assure sparger operability throughout fuel cycle 6.

External Pipe Clamp Fix

External sparger pipe clamps shall be designed so as to satisfy "full operability" requirements upon installation. The circumstances under which clamps will be installed over a crack in a local region on the sparger or jumper pipe are as follows:

1. In the event that crack arrest is not predicted for a given crack.
2. In the event that a crack indication is found or predicted to extend for 180^{o} in the circumferential direction in the field of view. It cannot be demonstrated by visual inspection methods that cracking does not continue around the backside of the pipe.
3. In the event that circumferential cracks are found at or near the top or bottom of the pipe within the field of view. It cannot be demonstrated by visual inspection methods that cracking does not continue around the backside of the pipe.
4. In the event that sparger design function and operability criteria are exceeded. (flow rate, momentum and spray pattern operability criteria are being developed).*
5. If a significant number of areas are determined to require clamping based upon the above criteria, an optional air test of the sparger assembly may be performed to identify areas of through-wall cracking.

Replace Sparger Assembly

Based upon present engineering knowledge, including empirical data and analytical model results, we do not predict or forsee any situation where the application of clamps will not provide a sound engineering fix. Clamping where warranted in local areas is considered to be the primary fix and the need for sparger replacement is not anticipated. However, the following maintenance criteria is proposed as a contingency.

Replacement of the sparger, or a sparger pipe segment, will be implemented only if clamping is not practical or feasible.

NOTE: APTECH has not performed a structural integrity evaluation nor operability/safety evaluations of the 304ss jumper pipe system. However, crack propagation studies performed for the sparger juncture box weld region are representative and applicable to jumper pipe welds which were not heat treated after welding.

* See pages 5-10.

APTECH ENGINEERING
SERVICES, INC.
795 SAN ANTONIO ROAD
PALO ALTO, CALIFORNIA 94303

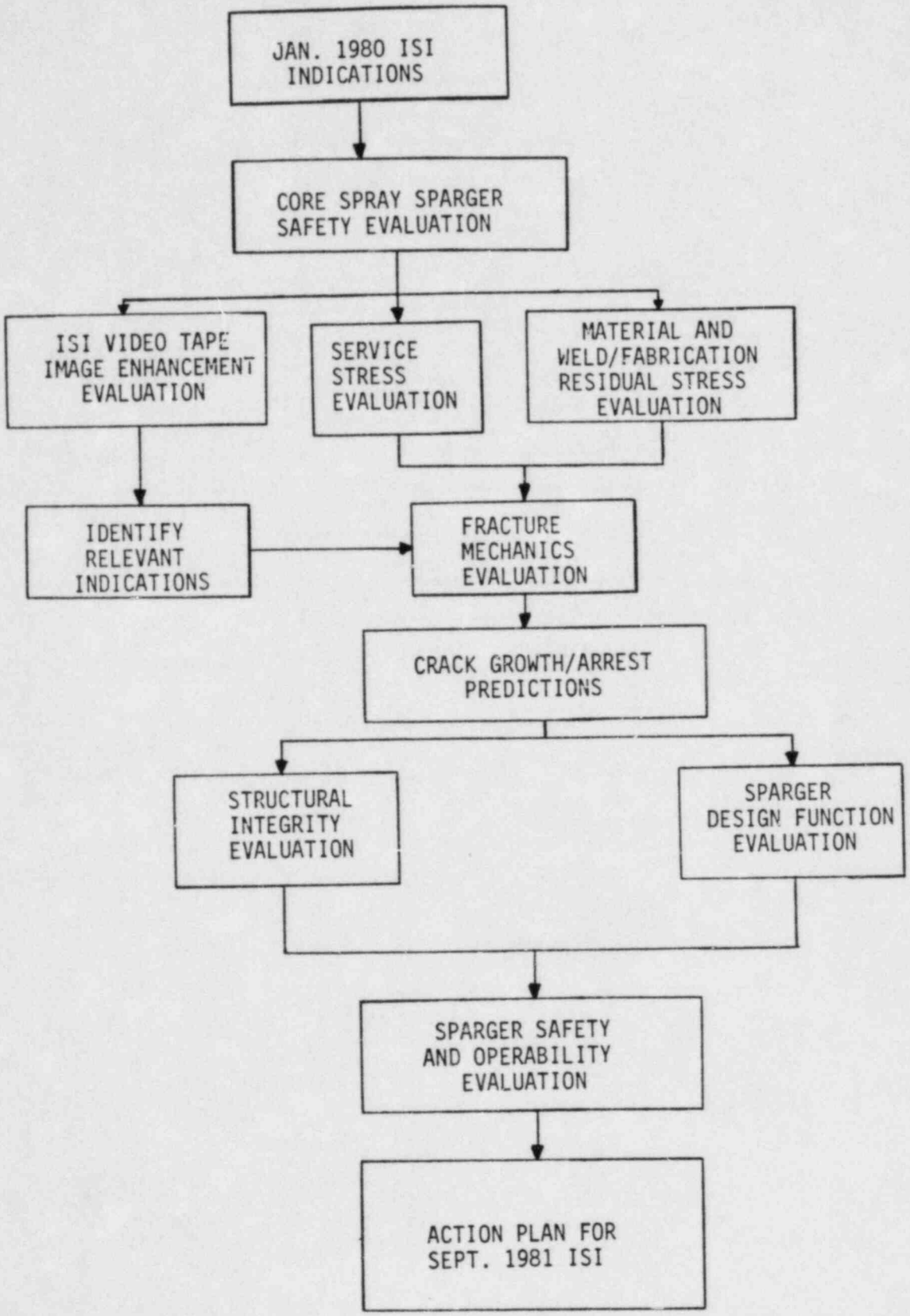

Figure 1 - Pilgrim Core Spray Sparger Evaluation Flow Chart

APTECH ENGINEERING
SERVICES, INC.
795 SAN ANTONIO ROAD
PALO ALTO, CALIFORNIA 94303

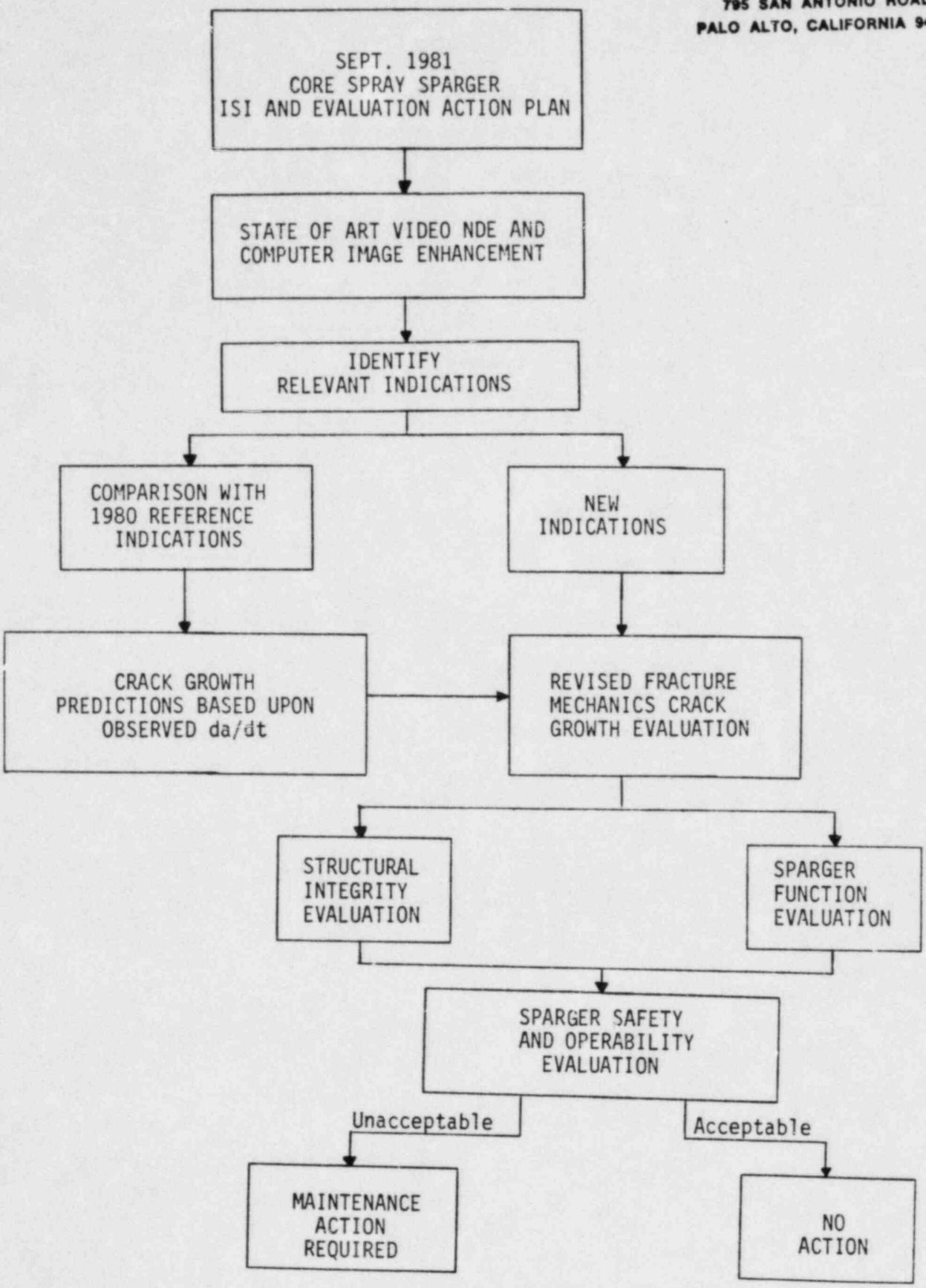

Figure 2 - Pilgrim Core Spray Evaluation Flow Chart

APTECH ENGINEERING
SERVICES, INC.
795 SAN ANTONIO ROAD
PALO ALTO, CALIFORNIA 94303

PROPOSED PILGRIM CORE SPRAY SPARGER EVALUATION PLAN

Sparger Function Evaluation

Sparger functional requirements include core reflood, heat transfer, sparger nozzle flow rates and sparger spray pattern. This evaluation study includes only the latter two items. The first two are being addressed by General Electric.

Sparger Nozzle Flow Rate

A fluid mechanics study was performed which considered the flow rate design requirements of 3600 gpm per sparger circle and the actual pump capacity reserve margin. Once those values were established, the pump system performance curves provided a basis for establishing the change in flow rates as a function of crack area.

Pump performance curves are shown in Figure 1. Figure 2 shows expanded pump curves in the area of interest. This figure illustrates that the reserve pumping capacity is approximately 20% greater (4300 gpm compared to 3600 gpm) than the design flow requirement for the case of no leakage, (i.e. when no cracks are present). However, as crack leakage increases, the calculations show that a maximum leakage flow of 1400 gpm (5000 gpm minus 3600 gpm) could be present and the pump would still provide flow through the nozzles at the design rated flow of 3600 gpm. For conservatism and to account for other system uncertainties, it is recommended that the leak criteria should be based upon half of the reserve pump capacity. The operating point would then be at point 3 in Figure 2. The nozzle flow would be about 3960 gpm, and the crack leakage would be 740 gpm.

Table 1 summarizes the evaluation and presents the results in a parametric form of acceptable crack length versus crack width, based upon 50% of the reserve pump capacity.

Table 2 shows the resulting clamp fix criteria. The system can tolerate a crack .010 in. wide and 57 feet long, which is equivalent to adding about 40 small nozzles to the sparger system. These calculations indicate that it is highly unlikely that crack clamping will be required because of insufficient flow capacity due to crack leakage.

Nozzle Spray Distribution

Fluid Mechanics calculations were performed to determine the relative effects of flow through a typical sparger nozzle as compared to a crack of varying length and width. Parametric calculations are summarized in Table 2 as a function of ratios of velocity, flow rate and momentum.

APTECH ENGINEERING
SERVICES, INC.
795 SAN ANTONIO ROAD
PALO ALTO, CALIFORNIA 94303

Sparger inspection data from Oyster Creek indicated that the largest measured circumferential crack was approximately .010 in. wide. A bounding evaluation was performed assuming that crack width and a circumferential crack 180° at the intrados, located between two of the smallest nozzles. The Rm value from Table 1, divided by the crack length, gives a momentum flow of approximately 35% of the magnitude for one Fulljet IM12 nozzle. Since there are 56 of these nozzles and 56 larger nozzles in each sparger circle, the effect of bounding crack flow is seen to be negligible and would be expected to affect spray distribution only in a local region within a radial distance of a few feet from the nozzle sparger.

Interference with nozzle spray pattern is only possible for through-wall cracks at the sparger intrados. Since structural criteria dictates that 180° cracks (5.5 in) shall be clamped, only smaller cracks at the sparger intrados need be considered.

Rather than postulating a bounding crack, consider a more realistic circumferential crack length of 4 inches as predicted by fracture mechanics analysis based upon measured residual stress distribution due to pipe fabrication. Since IGSCC cracks are inherrently tight, assume a crack width of .004 in. Calculated momentum flow from Table 1 is approximately 8% of the momentum flow of one Fulljet IM12 nozzle.

This study indicates that an individual crack will have a negligible effect on the core spray pattern. However, the spray pattern could be affected if a number of through wall cracks were present in a local region between two nozzles.

Proposed Clamp Fix Extension for Spray Pattern

An external pipe clamp will be installed over cracks when the cumulative crack lengths and widths result in total flow momentum equal to or greater than the flow momentum of the two adjacent nozzles.

APTECH ENGINEERING
SERVICES, INC.
795 SAN ANTONIO ROAD
PALO ALTO, CALIFORNIA 94303

CRACK WIDTH (INCH)	CRACK FLOW VELOCITY (FT/SEC)	10% RESERVE CAPACITY CRACK LENGTH * (INCH)
0.001	2.92	81,000
0.002	11.0	10,800
0.004	29.2	2,000
0.010	33.4	690
0.015	37.8	420

* Length needed for 740 GPM crack flow.

TABLE 1 Core Spray Sparger Pump Leak Rate Criteria

FIGURE 1

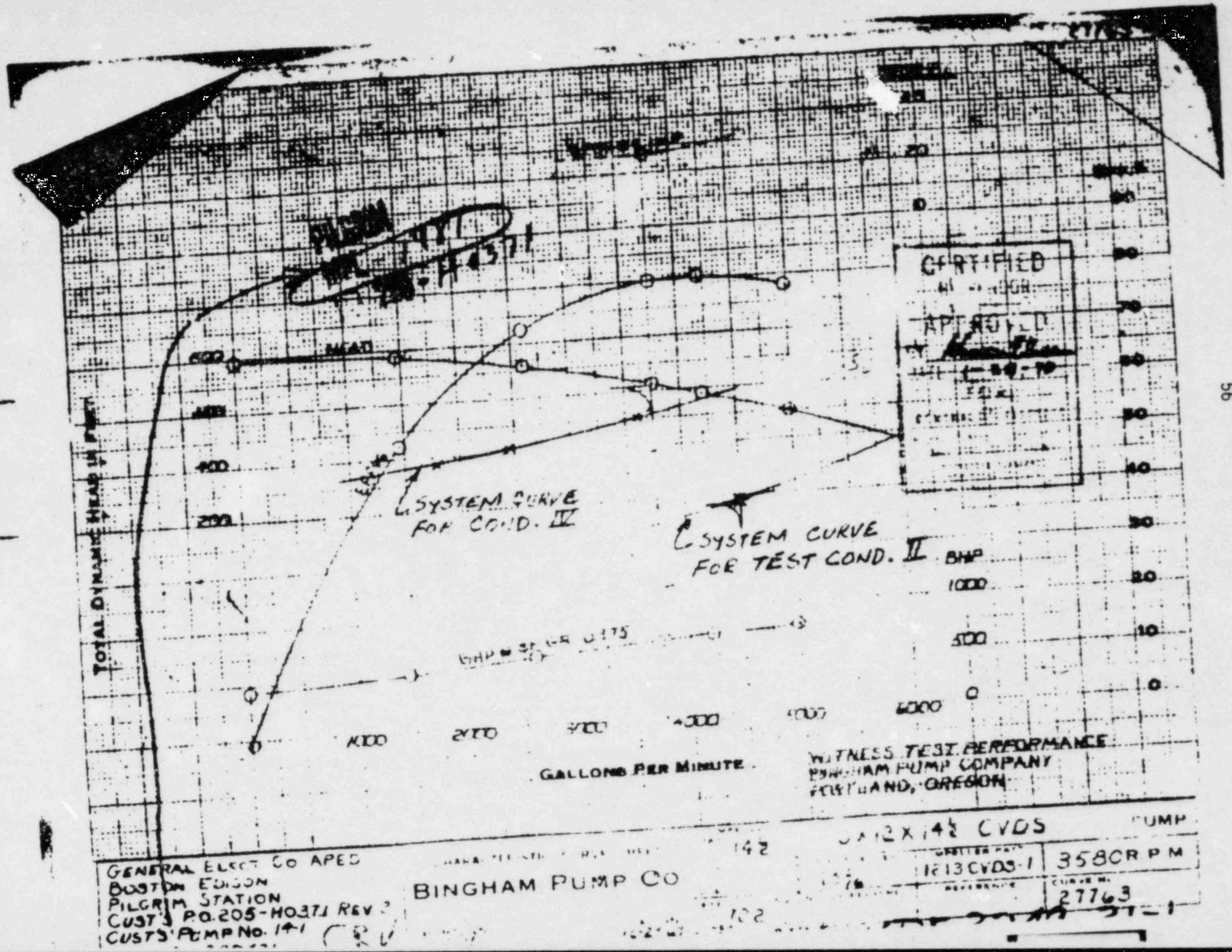
CERTIFIED
APPROVED
SYSTEM CURVE FOR COND. IV
SYSTEM CURVE FOR TEST COND. II
TOTAL DYNAMIC HEAD IN FEET
BHP
GALLONS PER MINUTE
WITNESS TEST PERFORMANCE
BINGHAM PUMP COMPANY
PORTLAND, OREGON
GENERAL ELECT CO APED
BOSTON EDISON
PILGRIM STATION
CUST'S P.O. 205-H0371 REV 3
CUST'S PUMP NO. 141
BINGHAM PUMP CO
12 X 14½ CVDS PUMP
12 13 CVDS-1
3580 R P M
27763

APTECH ENGINEERING
SERVICES, INC.
795 SAN ANTONIO ROAD
PALO ALTO, CALIFORNIA 94303

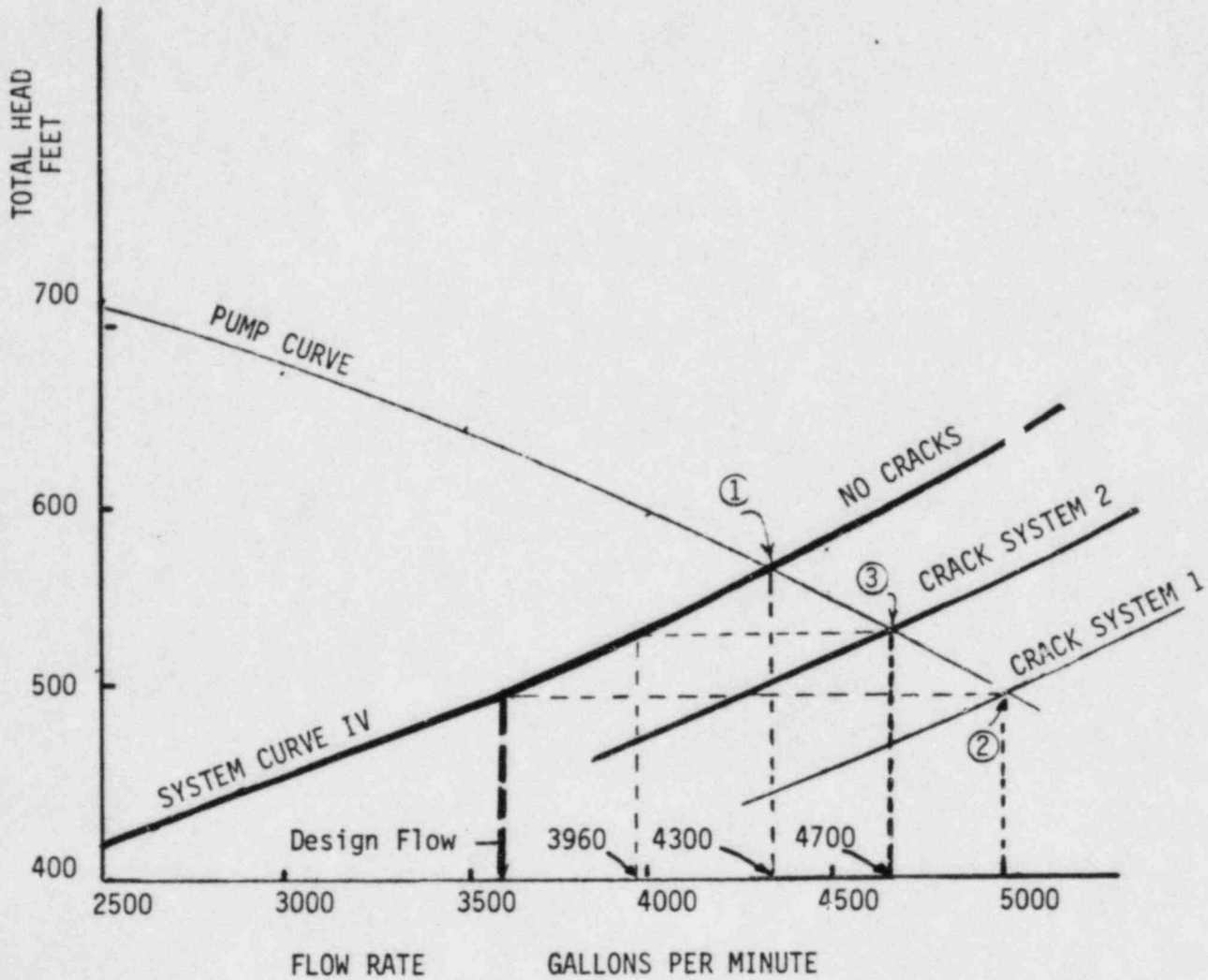

FIGURE 2 Pilgrim Core Spray System Pump Performance Curves

TABLE 2

PILGRIM CORE SPRAY SPARGER

Crack Leak Rate Evaluation

ASSUMPTIONS:

Nozzle: Pressure Drop = 15 psi
Flow* = 17.1 GPM = 0.0381 Ft.^{3}/sec.
Velocity = 31.7 Ft/sec.
Momentum Rate = 1.21 ρ LBM Ft./sec.^{2}
Where ρ = Density in LBM/Ft.^{3}

Crack: ΔP = 15 psi
Length : 1 inch
Depth : 0.226 inch

Crack Width inch	Velocity Crack Flow Ft./sec.	R_V	R_Q	R_M	Flow Type
0.001	2.92	10.9	1877	20,400	Laminar
0.002	11.0	2.9	249	712	Laminar
0.004	29.2	1.1	27	51.3	Laminar
0.010	33.4	0.95	16	15.6	Turbulent
0.015	37.8	0.84	9.7	8.1	Turbulent
0.025	41.8	0.76	5.4	4.0	Turbulent

R_V = Nozzle Velocity / Crack Velocity

R_Q = Nozzle Flow Rate / Crack Flow Rate

R_M = Nozzle Momentum Flow / Crack Momentum Flow

* : Fulljet Nozzle Catalog, page 14.
1M12 has 17.1 gal./min. @ 15 psi
Nozzle Orifice 15/32 in. dia.
(112 nozzles in two full circles)

APTECH ENGINEERING SERVICES, INC.
795 SAN ANTONIO ROAD
PALO ALTO, CALIFORNIA 94303